



Universidad Autónoma
de Madrid

Biblos-e Archivo
Repositorio Institucional UAM

Repositorio Institucional de la Universidad Autónoma de Madrid

<https://repositorio.uam.es>

Esta es la **versión de autor** del artículo publicado en:
This is an **author produced version** of a paper published in:

ACS Sustainable Chemistry and Engineering 11.17 (2023): 6498-6509

DOI: <https://doi.org/10.1021/acssuschemeng.2c05870>

Copyright: © 2023 American Chemical Society

El acceso a la versión del editor puede requerir la suscripción del recurso

Access to the published version may require subscription

COMPARISON OF NUTRIENT RELEASE STRATEGIES IN HYDROTHERMALLY TREATED DIGESTED SEWAGE SLUDGE

Andres Sarrion^{1*}, M. Angeles de la Rubia¹, Nicole D. Berge², Angel F. Mohedano¹, Elena Diaz¹

¹ Department of Chemical Engineering, Faculty of Sciences, Universidad Autonoma de Madrid, Campus de Cantoblanco, 28049, Madrid, Spain

² Civil and Environmental Engineering Dept., University of South Carolina, Columbia, 300 Main St., 29201, South Carolina, United States

*andres.sarrion@uam.es

Abstract

This work studies the fate of nutrients (N, P and K) during the hydrothermal treatment of anaerobically digested sewage sludge to raise their concentrations in the liquid phase and facilitate their recovery as solid mineral by chemical precipitation. The hydrothermal process has been optimized by evaluating temperature (170 – 230 °C) and reaction time (5 – 60 min) in an acid-free medium or with the addition of HCl (0.1 – 0.5 M). In the acid-free hydrothermal reactions, nutrients were mainly concentrated in the hydrochar, which were extracted with 0.5 M HCl (10% w/v). Following this route, 6.9 g N/kg, 13.8 g P/kg, and 8.8 g K/kg contained in the feedstock were extracted from the hydrochar produced at 230 °C, which considering direct nutrient solubilization to process water by acid-free HTT, accounts for 82, 83, and 78% N, P, and K release, respectively. In the HCl-assisted hydrothermal treatment, the release of nutrients directly into the process water was improved and depended mainly on the acid concentration used and to a lesser extent on the reaction temperature. Operating at 230 °C and 0.5 M HCl, a release of 98% N (more than 45% as NH₄-N), 87% P (as PO₄-P) and 70% K contained in the feedstock was achieved in the process water. Chemical precipitation of phosphorus and nitrogen from the process water allowed the recovery of a solid identified as crystalline struvite, with a high content in P, Mg, NH₄-N and negligible heavy metals

1
2
3 26 content. The estimated cost of digested sewage sludge treatment could reach 13.7 euros per
4
5 27 ton, considering the energy inputs required in the hydrothermal treatment.
6
7

8 28
9
10
11 29 **Keywords:** Biomass valorization, Digested sewage sludge, Hydrochar, Hydrothermal
12
13 30 carbonization, Nutrient solubilization.
14
15

16 31 **Abbreviation list**

17
18
19 32 AD, anaerobic digestion.
20
21

22 33 FC, fixed carbon.
23
24

25 34 HCT-[HCl], hydrochar, T represents reaction temperature (°C) and [HCl] the added HCl
26
27 35 concentration (M), if applicable.
28
29

30 36 HC-W, washed hydrochar
31
32

33 37 HHV, higher heating value.
34
35

36 38 HTT, hydrothermal treatment.
37
38

39 39 L-T, leachant from hydrochar acid washing, T represents reaction temperature (°C) for
40
41 40 hydrochar obtaining.
42
43

44 41 PWT-[HCl], process water, T represents reaction temperature (°C) and [HCl] the added HCl
45
46 42 concentration (M), if applicable.
47
48

49 43 RSM, response surface methodology.
50
51

52 44 VM, volatile matter.
53
54

55 45 W_{DSS} , digested sewage sludge weight.
56
57

58 46 W_{HC} , hydrochar weight.
59
60

1
2
3 47 W_{ST} , struvite weight.
4
5

6 48 W_{TSPW} , total solid weight in process water.
7
8

9 49 Y_{HC} , hydrochar mass yield.
10
11

12 50 Y_{PW} , process water yield.
13
14

15 51 Y_{ST} , struvite recovery yield.
16
17

18 52 **Introduction**

19
20
21 53 Anaerobic digestion (AD) is a widely used mature and economically viable technology that
22
23 54 biochemically transforms sewage sludge to biogas. The biogas is often used to obtain heat and
24
25 55 energy, improving the economic and environmental benefits of the process. Digested sludge is
26
27 56 generally stable and devoid of pathogens and odor¹. Importantly, digested sludge is an organic
28
29 57 waste that contains large amounts of nutrients (> 40 g N/kg; > 20 g P/kg; 5 g K/kg)²⁻⁴,
30
31 58 comparable to the nutrient content of other biomass wastes, such as animal manure (30 – 60 g
32
33 59 N/kg; 15 – 20 g P/kg; 10 – 25 g K/kg)⁵⁻⁷ and food waste (25 – 35 g N/kg; 3 – 6 g P/kg; 3 – 12
34
35 60 g K/kg)⁸⁻¹⁰. These nutrients represent the primary components found in agricultural fertilizers.
36
37 61 It is estimated that more than 250 million tonnes of fertilizers will be needed by 2050^{8,11}.
38
39 62 However, the scarcity of nitrogen and phosphorus naturally in the soil, in particular, has been
40
41 63 well-documented^{10,12,13}, prompting work evaluating options to replace their production from
42
43 64 natural sources, which are energetically and environmentally expensive¹³. Recovering the
44
45 65 phosphorus, nitrogen, and potassium found in digested sludge would be highly beneficial for
46
47 66 their use as a sustainable source of nutrients for fertilizers.
48
49
50
51
52

53
54 67 Hydrothermal treatments (HTT) have the potential to sustainably recover nutrients from wet
55
56 68 biomasses^{8,10,14,15}. Under hydrothermal carbonization conditions (180 – 250 °C and self-
57
58 69 generated pressure), wide range of wet biomasses, including digested sewage sludge, are
59
60

1
2
3 70 chemically transformed¹⁶. HTT process has been shown to be advantageous when compared
4
5 71 to other thermochemical processes such as pyrolysis¹⁷, gasification¹⁸ or combustion¹⁹, which
6
7 72 all require initial feedstock drying. More research is needed on HTT chemical reactions, the
8
9 73 kinetics, the effect of operating conditions and use of catalysts, energy and heat recovery,
10
11 74 combination with other technologies, and technical and economic aspects²⁰. The hydrothermal
12
13 75 process yields a carbonaceous solid, called hydrochar, with physical and energetic properties
14
15 76 similar to those of lignite coal; a process water, which acts as a solvent and contains a large
16
17 77 amount of organic compounds and mineral salts; and a small gaseous phase composed
18
19 78 primarily of CO₂²¹.

23
24 79 Hydrothermal treatment has been used to recover a variety of resources from wastes,
25
26 80 including nutrients. Many papers found in the literature have addressed the fate of nutrients
27
28 81 (N, P and K) during the HTT of wastes. Idowu et al. (2017)⁸ studied the nutrient recovery
29
30 82 from food waste (225 – 275 °C for 24 h) observing that most of the N remained integrated in
31
32 83 the hydrochar (> 50%), regardless of the reaction temperature, while the highest release of P
33
34 84 (70%) and K (96%) occurred at 225 °C and 4 h reaction time. In the case of digested sludge, a
35
36 85 lower temperature (170 °C for 1 h) allowed 80% release of the N to the process water,
37
38 86 yielding a P release lower than 40%¹⁵. Recent studies have also shown that HTT under acidic
39
40 87 conditions can enhance P leaching to process water^{5,7,10,22}, since most of the P is in the form
41
42 88 of insoluble inorganic P linked to multivalent metal elements (Fe, Ca, Al, Mg) present in the
43
44 89 feedstock. Acid-assisted HTT of animal manure showed that the addition of inorganic acids
45
46 90 (HCl, H₂SO₄) allowed the release of more than 95% of P and 60% of N at a lower acid
47
48 91 concentration than using organic acids (citric acid, acetic acid) at temperatures below 200
49
50 92 °C^{5,7,22}. Food waste has also been treated by acid-assisted HTT to solubilize nutrients in the
51
52 93 process water, being reported that more than 95% of N, P and K were solubilized using an
53
54 94 inorganic acid (0.5 M HCl) at 170 °C¹⁰.

1
2
3 95 Nutrient-rich process water could have potential use as a liquid fertilizer, with prior pH
4
5 96 conditioning being necessary²³. However, fertilization studies should be carried out to ensure
6
7 97 the suitability of the process water for plant growth, which can occasionally be negative due
8
9 98 to the presence of phytotoxic substances²⁴. Another possibility, once the nutrients have been
10
11 99 concentrated in the process water, is to recover them by physicochemical processes. P and N
12
13 100 are usually the main concern, and are commonly recovered as struvite by chemical
14
15 101 precipitation²⁵. Struvite obtained from biomass waste-derived solutions is more advantageous
16
17 102 and effective than a liquid fertilizer because of the high content of slow-release available P,
18
19 103 and low presence of pathogen and heavy metal²⁶. Becker et al. (2019)²⁷ hydrothermally
20
21 104 treated digestate at 180 °C in the presence of 2 M HNO₃ for 2 h and precipitated a struvite-
22
23 105 like solid by mixing PO₄-P rich hydrochar leachant, obtained by washing hydrochar with 2 M
24
25 106 citric acid in a 1:10 w:v ratio, and NH₄-N-rich process water. Zhang et al. (2020)²⁵ treated
26
27 107 swine manure digestate to HCl plus H₂O₂ assisted hydrothermal treatment at 60 – 180 °C for
28
29 108 15 – 45 min, and then the process water was derived to crystallization of a struvite-like solid.
30
31 109 Both studies used MgCl₂ as an ionic exchange reagent to set the molar ratio of PO₄:Mg:NH₄
32
33 110 to a value of 1:1.3:1 at pH 8.5-9. Sometimes the cost of these reagents is too high to ensure
34
35 111 the economic feasibility of the process. For this reason, other cheaper reagents are often used,
36
37 112 such as CaO, which allows the precipitation of apatite-like materials instead of struvite-like
38
39 113 ones²⁸.

40
41
42 114 Since nutrient solubilization in process water could be negatively affected by the presence of
43
44 115 inorganic elements⁸, the nutrient leaching pathway through acid washing of hydrochar has
45
46 116 been widely considered. However, little information exists on the behavior of nutrients over
47
48 117 the reaction time. This work aims to analyze the evolution of nutrients (N, P and K) and that
49
50 118 of other inorganic elements (Al, Ca, Fe and Mg) in process water over the reaction time, and
51
52 119 at different temperatures (170 – 230 °C) under acid-free and acid-assisted HTT (0.1 – 0.5 M
53
54
55
56
57
58
59
60

1
2
3 120 HCl), which could be advantageous in providing new routes for the management of a digested
4
5 121 sewage sludge containing large amounts of nutrients and inorganic elements, allowing to
6
7 122 understand about the interaction between them throughout the reaction. The main novelty of
8
9 123 this work lies in comparing nutrient solubilization between HCl-assisted HTT and that which
10
11 124 combines acid-free HTT with acid washing of hydrochar, for the subsequent nutrient recovery
12
13 125 of nutrients by chemical precipitation of struvite-like material. The hydrochar and struvite-
14
15 126 like material characterization results are expected to provide understanding on the conditions
16
17 127 necessary for its suitable use for industrial purposes.
18
19
20
21

22 128 **Materials and methods**

23 24 25 129 **Digested sewage sludge**

26
27
28 130 Digested sewage sludge was collected from a municipal wastewater treatment plant (located
29
30 131 in the north of the Community of Madrid, Spain), after mixed (primary plus secondary)
31
32 132 sewage sludge stabilization in a mesophilic anaerobic reactor, and subsequent dewatering
33
34 133 process. The feedstock was homogenized with an industrial mixer and stored in 1.5 kg
35
36 134 portions at -20 °C. Before use, the feedstock was defrosted and characterized, presenting a
37
38 135 moisture content close to 90 wt.%. The main characteristics of the digested sewage sludge
39
40 136 were: pH 8.2 ± 0.1 ; total solids, 101.8 ± 0.6 g/kg; volatile solids, 60.7 ± 0.8 g/kg; and total
41
42 137 chemical oxygen demand (TCOD), 84.2 ± 6.5 g/L. Proximate and elemental composition, and
43
44 138 HHV of dry feedstock are shown in **Table 1**. The composition of inorganic elements is
45
46 139 reported in the results and discussion section "Characterization of raw material and
47
48
49
50 140 hydrochars", and the content of the main heavy metals is shown in **Table S1**.

51 52 53 54 141 **Hydrothermal treatment**

55
56
57 142 HTT of digested sewage sludge was carried out in an electrically heated 316 ZipperClave
58
59 143 stainless steel pressure reactor, with a working volume of 4 L (Autoclave Engineers, USA). In
60

1
2
3 144 each experiment, the reactor was loaded with 1.5 kg of wet digested sewage sludge. The
4
5 145 operating temperature (170, 200, and 230 °C) was reached by heating the reactor at a rate of 3
6
7 146 °C/min and was maintained for 1 h. The impact of reaction temperature and acid
8
9
10 147 concentration (0.1, 0.3, and 0.5 M HCl, PanReac) on nutrient fate was studied. Response
11
12 148 surface methodology (RSM) based on a first-degree model was used to design the
13
14 149 experimental matrix used in this work to analyze the effect of temperature and acid addition
15
16 150 on the fate of nutrients during the HTT. RSM is a tool that has been used to determine optimal
17
18 151 HTT conditions for other pre-defined goals. In this work, an experimental matrix was
19
20 152 generated based on a central composite rotatable design with a duplicate of the central point.
21
22 153 Using Minitab 19 software, a matrix of 6 acid-assisted experiments (4 factorial point and 2
23
24 154 central point replicates) was generated. In addition, 3 acid-free experiments were also
25
26 155 performed. All the tests were performed by duplicate (amounting 12 and 6 reactions for HCl-
27
28 156 assisted and acid-free HTT, respectively).

29
30
31
32
33 157 For all experiments, reaction samples (40 mL) were withdrawn from the reactor at 5, 15, 30
34
35 158 and 60 min. Then, the reaction was stopped by cooling with an internal heat exchanger using
36
37 159 tap water. The resultant slurry was separated into solid (hydrochar) and process water by
38
39 160 filtration with a 250- μm membrane vacuum filter. The hydrochar was weighed after oven-
40
41 161 drying of the solid fraction overnight at 105 °C, with subsequent grinding and sieving to a
42
43 162 particle size between 100 and 200 μm . The liquid fraction was filtered with 0.45 μm Scharlab
44
45 163 glass filters and the obtained process water was stored at 4 °C. The hydrochar and process
46
47 164 water were labeled as HCT-[HCl] and PWT-[HCl], respectively, where T represents reaction
48
49 165 temperature (°C) and [HCl] the added HCl concentration (M), if applicable. The mass yield of
50
51 166 hydrochar (Y_{HC}) was calculated by **Eq. 1** and defined as the weight ratio of recovered
52
53 167 hydrochar (W_{HC}) to feedstock (W_{DSS}) on a dry basis.

54
55
56
57
58
59 168
$$Y_{\text{HC}} (\%) = (W_{\text{HC}}/W_{\text{DSS}}) \cdot 100 \quad (1)$$

1
2
3 169 Likewise, the process water yield (Y_{PW}) expresses the mass ratio of total solids in process
4
5 170 water (W_{TSPW}) to that of digested sewage sludge (W_{DSS}) on a dry basis, and was calculated
6
7
8 171 with Eq. (2):
9

$$10 \quad 172 \quad Y_{PW} (\%) = W_{TSPW}/W_{DSS} \quad (2)$$

13 173 **Nutrient leaching from plain hydrochar**

14
15
16
17 174 A hydrochar sample (5 g) from each acid-free run was mixed with 50 mL of 0.5 M HCl using
18
19 175 an orbital shaker (Julabo SW22, Germany) at 150 rpm for 2 h to evaluate the leaching of N, P
20
21 176 and K¹⁰. The resultant leachant (L-T) and the washed hydrochar (HC-W) were separated by
22
23 177 vacuum filtration (250 μ m). The leachant was filtered with 0.45 μ m Scharlab glass filter and
24
25 178 stored at 4 °C. Both leachant and washed hydrochar were subsequently analyzed using the
26
27
28 179 abovementioned methodology for process water and hydrochar.
29
30

31 180 **Nutrient recovery from process water**

32
33
34 181 A magnesium salt ($MgCl_2$) was added to a 50 mL sample of process water to promote the
35
36 182 struvite formation according to the molar ratio of Mg:PO₄ at 1.3:1²⁹. The mixture was basified
37
38 183 with 2 M NaOH up to pH 9 and kept under stirred for 20 min. The precipitated solid was
39
40 184 separated by filtration through 0.45 μ m and dried overnight at 105 °C, being labelled as ST (in
41
42 185 terms of struvite) followed to the HTT operating conditions (i.e., ST230, ST230-L or ST230-
43
44 186 A, where the term L refers to acid-free HTT plus leachant from hydrochar acid washing, and
45
46 187 the term A refers to HTT assisted by 0.5 M HCl). The struvite recovery yield (Y_{ST}) was
47
48 188 calculated by **Eq. 3** and defined as the weight ratio of recovered struvite (W_{ST}) to total solids
49
50 189 in process water (W_{TSPW}) in the precipitation step per process water yield (Y_{PW}) on a dry
51
52
53 190 basis.
54
55
56
57

$$58 \quad 191 \quad Y_{ST} (\%) = (W_{ST}/W_{TSPW}) \cdot Y_{PW} \quad (3)$$

192 Analytical methods

193 The elemental composition (C, H, N and S) of the feedstock, process water, leachant from
194 char washing, and hydrochar samples (including HC-W) was determined by duplicate on a
195 CHNS analyzer (LECO CHNS-932). A proximate analysis by thermogravimetry, according to
196 ASTM methods D3173-11, D3174-11, and D3175-11, was performed by duplicate to
197 determine the moisture, ash, volatile matter (VM) content and fixed carbon (FC) (by
198 difference), respectively, of the feedstock and hydrochar. The higher heating value (HHV) of
199 the dried feedstock and hydrochar was determined by **Eq. 4**, an unified correlation to
200 calculate the HHV from C, H, N, S, O and ash content (in wt.%) according to Channiwala et
201 al. (2002)³⁰.

$$\begin{aligned} 202 \text{ HHV (MJ/kg)} \\ 203 &= 0.349 \cdot C + 1.178 \cdot H + 0.100 \cdot S - 0.103 \cdot O - 0.015 \cdot N - 0.021 \cdot \text{Ash} \quad (4) \end{aligned}$$

204 The concentration of inorganic elements in the feedstock, hydrochar and process water was
205 determined by inductively coupled optical emission spectroscopy (ICP-OES) on an IRIS
206 INTREPID II XDL instrument from ThermoFisher Scientific. Solid samples were firstly
207 digested in a microwave digester using a mixture of hydrochloric acid, nitric acid and
208 hydrogen peroxide. The Standards Measurements and Testing (SMT) protocol, a sediment P
209 fractionation method, harmonized and validated in the frame of the standards, measurements
210 and testing program³¹, was applied to the HC-W to analyze P speciation (organic and
211 inorganic P)²⁹. Total P was obtained by mixing 0.2 g of hydrochar (previously calcined at 450
212 °C for 3 h) with 20 mL of 3.5 M HCl under continuous stirring at room temperature for 16 h.
213 Orthophosphate (PO₄-P) was determined by mixing 0.2 g of hydrochar with 20 mL of 1 M
214 HCl under continuous stirring at 25 °C for 16 h⁴. Total P and PO₄-P from supernatant and
215 those from process water were analyzed photometrically with a Hach Lange LCK350 cuvette
216 test. In the process water, NH₄-N content was assessed by distillation and titration according

217 to the standard method 4500-NH₃-B-C published by the American Public Health
 218 Association³². Nitrite (NO₂-N) and nitrate (NO₃-N) were quantified on a Dionex ICS-900 ion
 219 chromatograph with chemical suppression, fitted with a 4 × 250 mm Dionex IonPac AS22
 220 column, using a 1 mL/min mobile phase of 1.4/4.5 mM NaHCO₃ and Na₂CO₃. The results
 221 corresponding to P and N solubilization were also expressed as grams of P or N per kg of dry
 222 feedstock.

223 Results and discussion

224 Characterization of digested sewage sludge and hydrochar

225 **Table 1** includes the proximate and ultimate analysis of the feedstock and hydrochar,
 226 including those obtained after acid washing step. Digested sewage sludge showed a nutrient
 227 content of 28.4 g P/kg, 56.2 g N/kg, and 32.7 g K/kg on a dry basis, and a remarkable ash
 228 content (around 30 wt.%) attributed to the presence of Al (0.1 g/kg), Ca (20.1 g/kg), Mg (4.4
 229 g/kg) and Fe (47.0 g/kg) (d.b.).

230 **Table 1.** Main characteristics of digested sewage sludge and hydrochar^a on a dry basis.

Sample	Proximate analysis (wt.%)				Ultimate analysis (wt.%)					HHV (MJ/kg)
	Yield	FC	VM	Ash	C	N	S	H	O	
Digested sludge	-	10.8 (0.3)	59.4 (0.4)	29.8 (0.2)	30.5 (0.3)	5.6 (0.1)	1.4 (0.1)	4.6 (0.1)	28.1 (0.1)	12.6
HC170	76.4	11.1 (0.2)	49.9 (0.3)	39.0 (0.1)	28.3 (0.1)	3.7 (0.1)	1.1 (0.1)	4.2 (0.1)	23.7 (0.1)	11.5
HC200	57.6	11.3 (0.1)	45.3 (0.8)	43.4 (0.1)	27.7 (0.1)	3.3 (0.1)	1.2 (0.1)	3.9 (0.1)	20.5 (0.1)	11.4
HC230	57.1	11.4 (0.1)	43.9 (0.1)	44.7 (0.1)	27.3 (0.2)	3.0 (0.1)	0.7 (0.1)	3.9 (0.1)	20.4 (0.1)	12.5
HC170-W	50.8 ^b	19.2 (0.1)	70.3 (0.1)	10.5 (0.1)	42.7 (0.6)	2.6 (0.1)	0.4 (0.1)	5.1 (0.1)	38.7 (0.1)	18.1
HC200-W	39.7 ^b	18.7 (0.1)	71.2 (0.1)	10.1 (0.1)	52.3 (0.2)	2.1 (0.1)	0.2 (0.1)	5.9 (0.1)	29.4 (0.1)	21.9
HC230-W	40.1 ^b	19.0 (0.1)	71.3 (0.1)	9.7 (0.1)	52.4 (0.1)	2.0 (0.1)	0.2 (0.1)	5.7 (0.1)	30.0 (0.1)	21.9
HC170-0.1	53.7	12.1 (0.5)	50.2 (0.1)	37.7 (2.3)	28.4 (0.1)	3.7 (0.1)	1.0 (0.1)	4.1 (0.1)	25.1 (0.1)	11.3
HC170-0.5	25.9	16.7 (0.3)	48.3 (0.1)	35.0 (0.7)	30.9 (0.4)	3.3 (0.1)	0.9 (0.1)	4.2 (0.1)	25.7 (0.1)	12.4
HC200-0.3	31.9	12.6 (0.1)	47.4 (0.1)	40.0 (0.1)	31.2 (0.6)	3.5 (0.1)	0.8 (0.1)	4.2 (0.1)	20.3 (0.1)	13.2
HC230-0.1	51.4	12.5 (0.2)	47.4 (0.1)	40.1 (0.3)	31.5 (0.6)	3.5 (0.1)	1.0 (0.1)	4.2 (0.1)	19.7 (0.1)	13.1
HC230-0.5	31.5	17.4 (0.1)	43.9 (0.1)	38.7 (0.1)	29.1 (0.2)	2.3 (0.1)	1.2 (0.1)	3.8 (0.1)	24.9 (0.1)	12.7

231 Standard deviation is reported in brackets.

232 ^a Data obtained after 60 min reaction time.

1
2
3 233 ^b Values obtained considering mass hydrochar yield and mass lost due to acid washing.
4
5
6 234 The hydrochar yield was mainly influenced by temperature, decreasing by 19 percentage
7
8 235 points when the temperature increased from 170 °C to 200 °C in acid-free HTT experiments.
9
10 236 This fact could be explained by the effect of temperature on the degradation of organic
11
12 237 compounds of the digested sludge and their subsequent release into the process water¹². In the
13
14 238 case of acid-assisted HTT, the decrease in Y_{HC} (by 22 – 26 percentage points) is accentuated
15
16 239 by the role of strong acids to facilitate the solubilization of organic compounds⁶. In addition,
17
18 240 acid played a remarkable role in the solubilization of inorganic matter, leading to a decrease
19
20 241 in the hydrochar ash content, which accounts around 40 – 50% of the lost yield of hydrochar
21
22 242 with respect to acid-free HTT. This fact is also observed in the HC-W (decreasing by 17 – 26
23
24 243 percentage points but being this Y_{HC} related to that reported for acid-free hydrochars plus the
25
26 244 weight lost obtained after washing step).
27
28
29
30
31 245 The fixed carbon content in hydrochar did not vary throughout the acid-free HTT (10.8% in
32
33 246 the feedstock to 11.1 – 11.4% in HC170, HC200, and HC230), but the volatile matter content
34
35 247 decreased by about 16 percentage points under the same conditions. This evolution is related
36
37 248 to the decrease of C, H and O content of hydrochar because of decarboxylation and
38
39 249 dehydration of organic compounds (e.g. alcohols or ketones) of the feedstock ²⁵. Ash content
40
41 250 increased by 10, 13 and 15 percentage points in HC170, HC200 and HC230, respectively.
42
43
44
45 251 HTT temperature increased the solubilization of N and S in the process water, thus decreasing
46
47 252 their content in the hydrochar by 47 and 50%, respectively, at 230 °C. In the case of acid-
48
49 253 assisted HTT, a similar trend was observed with temperature of the main characteristics of
50
51 254 hydrochar, although strongly influenced by the acid concentration used. Acid washing of
52
53 255 hydrochar from acid-free HTT promoted the increase in fixed carbon and volatile matter
54
55 256 content and ash solubilization, obtaining materials with around 30 percentage points less ash
56
57 257 than the original hydrochar, without remarkable differences obtained at different
58
59
60

1
2
3 258 temperatures. Likewise, the N and S contents of the HC-W were substantially reduced to
4
5 259 values below 3 and 0.5%, respectively, resulting in hydrochar with the highest HHV values.
6
7
8 260 In general, the effect of acid seems to depend on how it is used. Added HCl during HTT
9
10 261 seemed to mainly influence the organic matter solubilization, because of the catalytic effect of
11
12 262 acid on hydrolysis, dehydration and condensation reactions, but did not prevent ash
13
14 263 agglomeration. However, HCl positively affected hydrochar ash removal during acid washing
15
16
17 264 step but did not show volatile matter solubilization, because of under non-hydrothermal
18
19 265 conditions, HCl mainly solubilizes phosphates and carbonates from the structure of the
20
21 266 hydrochar³³.
22
23
24 267 The characteristics of the hydrochar were compared with the values established by ISO
25
26
27 268 17225-8 for the use of thermally treated and densified biomass fuels. This standard indicates
28
29 269 that the HHV of digestate-based hydrochar should reach 18 MJ/kg and contain no more than
30
31 270 2% N, 0.2% S, 10% ash and 75% volatile matter. Therefore, only HC-W have the potential to
32
33
34 271 be used directly as solid fuels for industrial use. In a different way, hydrochar was evaluated
35
36 272 as crop support and soil amendment according to Regulation (EU) 2019/1009³⁴ on fertilizing
37
38 273 products, which establishes a minimum dry mass content of 20 wt.%, organic carbon content
39
40 274 of 7.5 wt.%, and specifies metal concentration limits for the application on various soils of
41
42 275 these hydrochars, which are as follows (in mg/kg): As < 40, Cd < 1.5, Cr < 2, Cu < 200, Hg <
43
44 276 1, Ni < 50, and Pb < 120. Therefore, those hydrochars from acid-free HTT would be suitable
45
46
47 277 as a solid organic fertilizer because they contain N, P, and K, and those from HCl-mediated
48
49 278 HTT would be suitable as soil amendment (nutrients have been mostly extracted) (**Table S1**).
50
51
52 279 However, beyond complying with the limits established by current regulations, some authors
53
54 280 have reported that the presence of certain organic compounds in hydrochars could inhibit
55
56
57 281 plant growth, highlighting the importance of conducting studies to ensure proper synergy
58
59 282 between HTC products and plant metabolism^{35,36}. Eskandari et al. (2019)³⁷ tested the effects
60

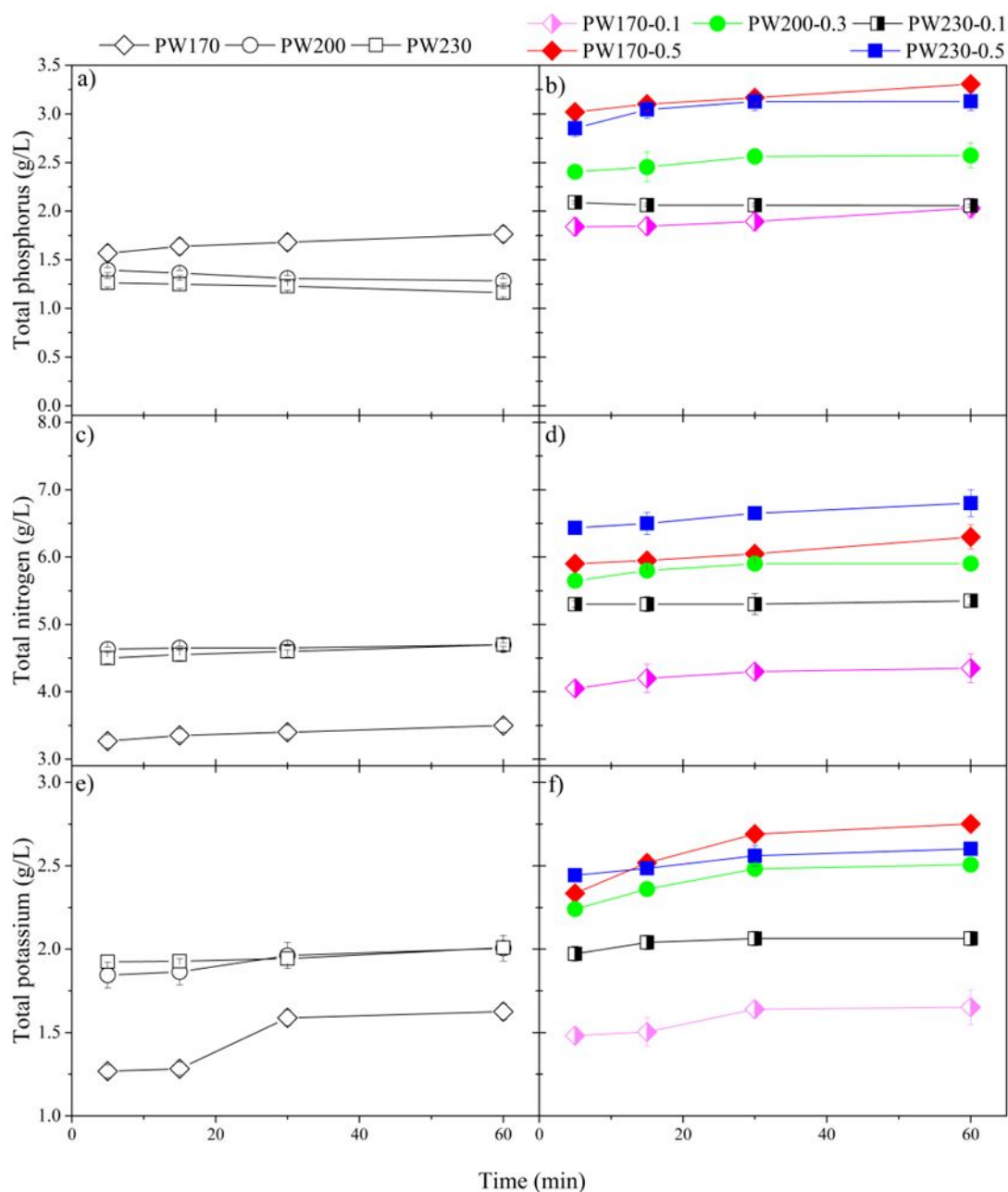
1
2
3 283 of paper mill sludge-based hydrochar on pine seedling growth and reported that the
4
5 284 application of adequate rates of hydrochar can reduce fertilizer requirements and showed
6
7 285 positive effects on germination, shoot biomass and stem diameter compared with control
8
9 286 seedlings (without hydrochar) under the fertilizer levels tested.”
10
11
12

13 287 **Nutrient release in process water**

14 15 16 288 **Fate of phosphorus**

17
18
19 289 **Fig. 1** shows the evolution of P concentration (as $\text{PO}_4\text{-P}$) in the process water during the
20
21 290 hydrothermal reactions. All the P in the process water was detected as PO_4^{3-} . In acid-free HTT
22
23 291 (**Fig. 1a**), the maximum P concentration (equivalent to 13.9 g P/kg feedstock) was reached at
24
25 292 170 °C after 60 min reaction time. In contrast, at 230 °C, the P concentration slightly
26
27 293 decreased with time, obtaining a concentration of 1.2 g P/L (equivalent to 9.7 g P/kg
28
29 294 feedstock) at the same reaction time. An increase in temperature favors hydrothermal
30
31 295 mechanisms and plays a key role in the fate of phosphorus, keeping it retained in the
32
33 296 hydrochar^{38,39}. During HTT, hydrolysis, decarboxylation and polymerization reactions occur,
34
35 297 promoting the hydrolysis of organic polyphosphates into orthophosphate (PO_4^{3-}). As a result,
36
37 298 metal cations such as Al^{3+} , Ca^{2+} , $\text{Fe}^{2+/3+}$ and Mg^{2+} show affinity for the PO_4^{3-} anion and leads
38
39 299 to the formation of complexes⁴⁰. Increasing temperature increases the crystallinity of these
40
41 300 metal phosphates by reducing their solubility⁴¹, which explains the decrease of P
42
43 301 concentration in the process water and the consequent increase of P in hydrochar (14.1 and
44
45 302 18.6 g P/kg feedstock in HC170 and HC230, respectively). This effect of temperature has
46
47 303 been previously described by Becker et al. (2019)²⁷, who hydrothermally treated a digested
48
49 304 sewage sludge observing that P solubilization in the process water at 220 °C was 14% lower
50
51 305 than at 190 °C. To analyze the effect of the presence of dissolved metal cations, **Fig. 2a** and
52
53 306 **2b** show the evolution of Al^{3+} , Ca^{2+} , $\text{Fe}^{2+/3+}$ and Mg^{2+} in the process water in acid-free HTT at
54
55
56
57
58
59
60

1
2
3 307 170 and 230 °C, respectively. At 170 °C, the concentration of Al^{3+} , Ca^{2+} , $\text{Fe}^{2+/3+}$ and Mg^{2+}
4
5 308 slightly increases during the reaction, which is equivalent to a total concentration of 8.1×10^{-3}
6
7 309 mol/L. This trend is similar to the trend obtained with P at that temperature (about 6.3×10^{-3}
8
9 310 mol P/L was solubilized in the process water). According to the molar ratios of phosphates
10
11 311 that can be formed with these metallic elements (Al:P (1:1), Ca:P (3:2), Fe:P (1:1 or 3:2,
12
13 312 depending to the Fe oxidation state), and Mg:P (3:2)), an excess of solubilized P in the
14
15 313 process water (around 1.3×10^{-3} mol P/L) not related with solubilization of metal phosphates
16
17 314 exists. This excess P may be associated with organic P from the hydrolysis of organic matter
18
19 315 (e.g. proteins, amino-acids) present in feedstock. At 230 °C, the concentration of all cations
20
21 316 decreased with time, similar to that of P. The drop in metal cation concentration (equivalent to
22
23 317 a total of 1.5×10^{-2} mol/L) is similar to the drop in the P concentration (equivalent to 1.8×10^{-2}
24
25 318 mol/L), suggesting it is feasible to that the P drop is related to the formation of insoluble
26
27 319 phosphates precipitated on the hydrochar⁴². Marin-Batista et al. (2020)⁴ worked on HTT of
28
29 320 digested sewage sludge observed a higher release of organic P to the process water as $\text{PO}_4\text{-P}$,
30
31 321 related to the increasing temperature. The solubilized $\text{PO}_4\text{-P}$ reacted with other inorganic ions
32
33 322 to form phosphate salts. In this way, higher HTT temperature resulted in an increase in
34
35 323 inorganic P in the hydrochar (about 80% of the total P appears in the hydrochar)⁴.
36
37
38
39
40
41
42
43
44
45
46
47
48
49
50
51
52
53
54
55
56
57
58
59
60

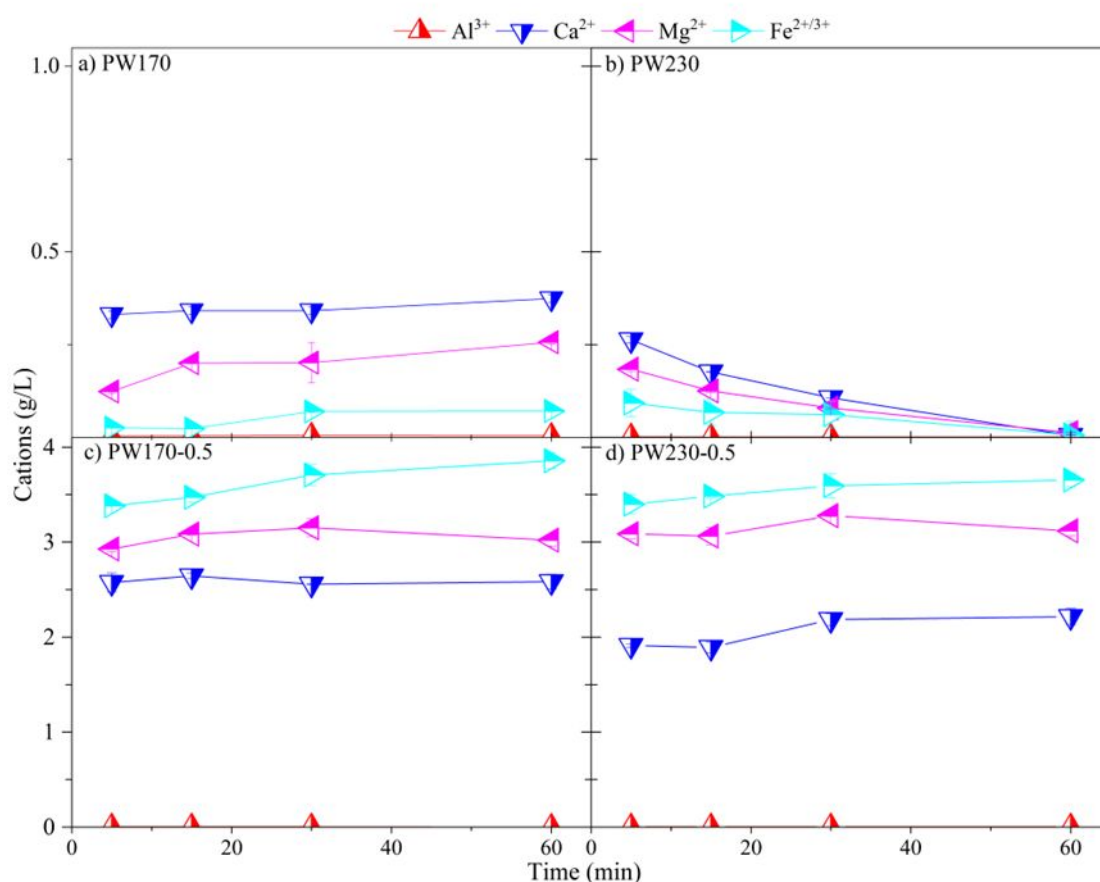


324
325 **Fig. 1.** Time course of phosphorous, nitrogen and potassium in process water for acid-free (a,
326 c and e) and HCl-assisted HTT (b, d and f).

327 In the case of HCl-assisted HTT (**Fig. 1b**), the P concentration in PW170-0.5, PW200-0.3,
328 and PW230-0.5 slightly increased with reaction time, while remained almost constant in
329 PW170-0.1 and PW230-0.1. The leaching of P from the solid to the process water increased
330 with increasing HCl concentration, showing no significant differences with temperature, and
331 reaching maximum values of 3.0 and 3.1 g P/L (equivalent to 24.9 and 25.5 g P/kg feedstock)

1
2
3 332 after 60 min reaction time at 170 and 230 °C, respectively, at the highest HCl concentration
4
5 333 (0.5 M). This observation is likely due to the fact that mineral acids facilitate the
6
7 334 transformation and dissolution of organic P (mainly proteins and amino acids) contained in
8
9 335 the digested sewage sludge and its subsequent release to process water^{5,7,43}. Attending to
10
11 336 literature, not only the acid concentration but also the type of acid and the characteristics of
12
13 337 the feedstock seem to have an influence on the P release. In the case of manure wastes, most
14
15 338 of the P appears as organic P (proteins, lipids, among others), which is easily hydrolyzable at
16
17 339 acidic pH, regardless of the type of acid used. This observation suggests that the addition of
18
19 340 organic or inorganic acids that result in a low pH value may be enough to solubilize most of P
20
21 341 in the process water. Qaramaleki et al (2020)⁷ indicated that almost all the P contained in a
22
23 342 fresh animal manure was leached into the process water using 0.5 M citric acid or 0.5 M HCl
24
25 343 at 170 °C. However, P from biomasses such as sewage sludge or digestates (from sewage
26
27 344 sludge, animal manure or agri-food wastes) usually appear as inorganic complexes⁴⁴,
28
29 345 requiring a strong inorganic acid to promote the solubilization of these complexes. Rodriguez
30
31 346 Correa et al. (2017)⁴⁵ reported that citric acid-assisted HTT of digested sewage sludge
32
33 347 evolved to new acids that did not promote P solubilization. Becker et al. (2017)²⁷
34
35 348 hydrothermally carbonized digested sewage sludge at 190 °C, previously acidified at pH 4.0
36
37 349 by addition of HNO₃, and observed that P was mainly retained in the hydrochar, indicating
38
39 350 that the pH of the process water after reaction was 4.8, which was not enough to achieve
40
41 351 solubilization of PO₄-P. In the present study, a positive effect of HCl addition on metal
42
43 352 solubilization was observed (**Fig. 2c** and **2d**), showing that acidic conditions (pH 3.1 and 2.8
44
45 353 at 170 °C and 230 °C, respectively) do not favor the formation of precipitable metal
46
47 354 phosphates. This is mainly due to the effect of pH on the phosphate species present in the
48
49 355 medium. At pH values below 4.8, phosphate anions were mainly in their monobasic form
50
51 356 (H₂PO₄⁻), which facilitates the formation of acid phosphates with cations such as Al³⁺, whose
52
53
54
55
56
57
58
59
60

357 bonding is favored by the decrease amount in OH^- anions⁴⁶. However, the formation of
 358 phosphates with divalent cations such as Ca^{2+} , $\text{Fe}^{2+/3+}$ or Mg^{2+} is not favored at very acidic pH
 359 values (< 4.8) because a decrease in the oversaturation of the medium occurs as a result of
 360 protonation of the dibasic phosphate species (HPO_4^{2-})⁴⁷. In the present study, an increase in
 361 the concentration of divalent cations and $\text{Fe}^{2+/3+}$ was observed in the process along the 0.5 M
 362 HCl-assisted HTT (equivalent to 1.3×10^{-2} and 1.4×10^{-2} mol/L at 170 °C and 230 °C,
 363 respectively), together with a slight drop in Al^{3+} concentration (equivalent to 6.4×10^{-5} and
 364 5.0×10^{-5} mol/L at the mentioned reaction temperatures), which can be related to the increase
 365 in P concentration (equivalent to 9.2×10^{-3} and 8.9×10^{-3} mol/L at 170 °C and 230 °C,
 366 respectively) to explain this trend.



368
 369 **Fig. 2.** Time course of main cations in the process water.

370 **Fate of nitrogen**

371 The fate of N during HTT of digested sewage sludge was analyzed by evaluating the
372 evolution of N concentration in the process water corresponding to acid-free and HCl-assisted
373 HTT (**Fig. 1c** and **1d**). In the acid-free HTT systems (**Fig. 1c**), the effect of temperature under
374 hydrothermal conditions favored the hydrolysis of proteins, amino acids, and multi-peptides
375 present in the feedstock, resulting in the release of different N compounds to the process
376 water⁴⁸. N release was remarkable above 200 °C (with similar values at 200 and 230 °C),
377 obtaining a N concentration of approximately 38.5 g N/kg feedstock. This value is 39%
378 higher than that obtained at 170 °C (27.9 g N/kg feedstock).

379 In the case of HCl-assisted HTT (**Fig. 1d**), an increase in N release with reaction time was
380 observed in most of cases except for PW230-0.1, where N concentration remained constant,
381 promoting the addition of acid a more positive effect than the increase in temperature. With
382 the addition of 0.1 M HCl, a 15% increase in the maximum N concentration in the process
383 water obtained at 170 °C and 230 °C (equivalent to 36.5 and 44.5 g N/kg feedstock,
384 respectively) was found compared to that obtained in acid-free reactions. Similarly, an
385 increase in HCl concentration appeared to favor N solubilization, with a maximum N
386 concentration of 6.8 g/L (55.4 g N/kg feedstock) at 230 °C and 0.5 M HCl. These results are
387 in accordance with those reported by others. Dai et al. (2017)²² concluded that an increase in
388 HCl concentration (0.25 – 2%) in the hydrothermal treatment of animal manure favored N
389 solubilization (from 1.6 to 2.6 g N/L). Also, Zhang et al. (2019)⁴⁹ reported that increasing the
390 temperature from 160 to 260 °C in acidic conditions (2% HCl) was essential for maximizing
391 the release of N (up to 85%) from corn stover to process water, while Qaramaleki et al.
392 (2020)⁷ observed that the best N leaching from animal manure into the process water was
393 obtained at temperatures above 200 °C using 0.5 M HCl (approximately 60% N from the
394 feedstock was solubilized in the process water).

1
2
3 395 An analysis of nitrogen species in the process water (**Fig. 3**) revealed concentrations of
4
5 396 organic N, NH₄-N, NO₃-N and NO₂-N equivalent to the total nitrogen in the feedstock.
6
7 397 Increasing the temperature from 170 to 230 °C along the acid-free reactions resulted in a 73
8
9
10 398 and 95% increase in organic N and NO₃-N, respectively, in the process water. Some studies
11
12 399 suggest that an increase of temperature enhances N solubilization to the process water, while
13
14 400 organic and inorganic nitrogen-bearing species undergo hydrolysis to generate NH₄-N and
15
16 401 NO₃-N^{50,51}. However, the increase in NH₄-N is less evident because the hydrolysis of organic
17
18 402 N (mainly as proteins and amino-acids) and its subsequent deamination to form NH₄-N is a
19
20
21 403 slow step at temperatures below 200 °C^{52,53}.

22
23
24 404 In HCl-assisted HTT, a significant effect of acid concentration on the solubilization of organic
25
26 405 N to process water was observed. Thus, in HTT assisted with 0.1 M HCl at 170 and 230 °C,
27
28 406 the solubilized organic N was 220% and 43% higher than in acid-free HTT, respectively,
29
30 407 while in HTT assisted with 0.5 M HCl, the organic N solubilization was even higher (430% at
31
32 408 170 °C and 230% at 230 °C) than plain HTT. Furthermore, increasing the reaction
33
34 409 temperature increased the transformation of organic N to NH₄-N (with a maximum value of
35
36 410 26.1 g NH₄-N/kg feedstock at 230 °C and 0.5 M HCl) was observed. The NO₃-N
37
38 411 concentration was largest at higher temperatures, but decreased with increasing HCl
39
40 412 concentration because deamination to form NH₄-N is promoted under acidic conditions⁵,
41
42 413 while the NO₂-N concentration was lower than 0.1% in all cases.
43
44
45
46
47
48
49
50
51
52
53
54
55
56
57
58
59
60

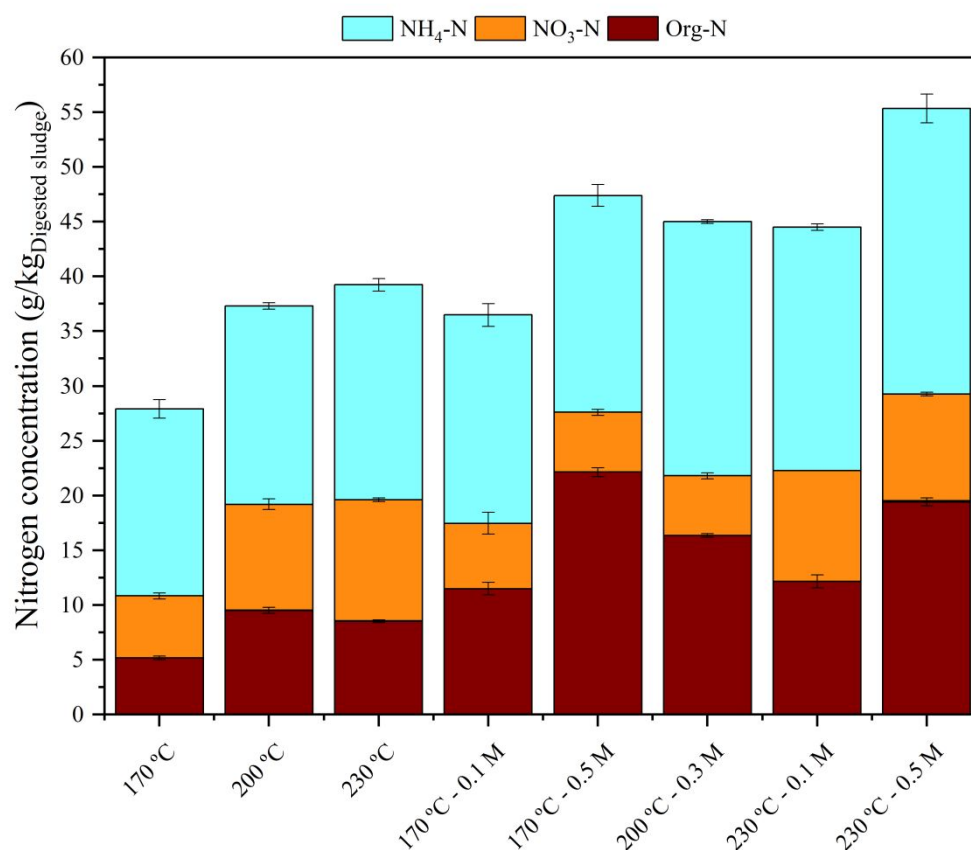


Fig. 3. Distribution of nitrogen species in the HTT process water after 60 min reaction time.

Fate of potassium

The leaching of K in the process water in acid-free HTT (**Fig. 1e**) increased with temperature and reaction time, increasing the K concentration by 25% at 60 min of reaction at 200 – 230 °C with respect to 170 °C. The addition of 0.1 M HCl in HTT (**Fig. 1f**) did not influence the K release compared to the results obtained in acid-free HTT. This could be related to the easy solubilization of K salts before medium saturation. Higher K solubilization was observed with the addition of 0.5 M of HCl, regardless of reaction temperature, because of an increase in K solubilization with decreasing pH. In general, total K solubilization is achieved after HTT of different biomass wastes (animal manure, microalgae, food waste, agricultural-digestate)^{8,15,54}, but in the case of digested sewage sludge, the high K concentration in the feedstock (32.7 g K/kg), reduced its total release because the equilibrium between all

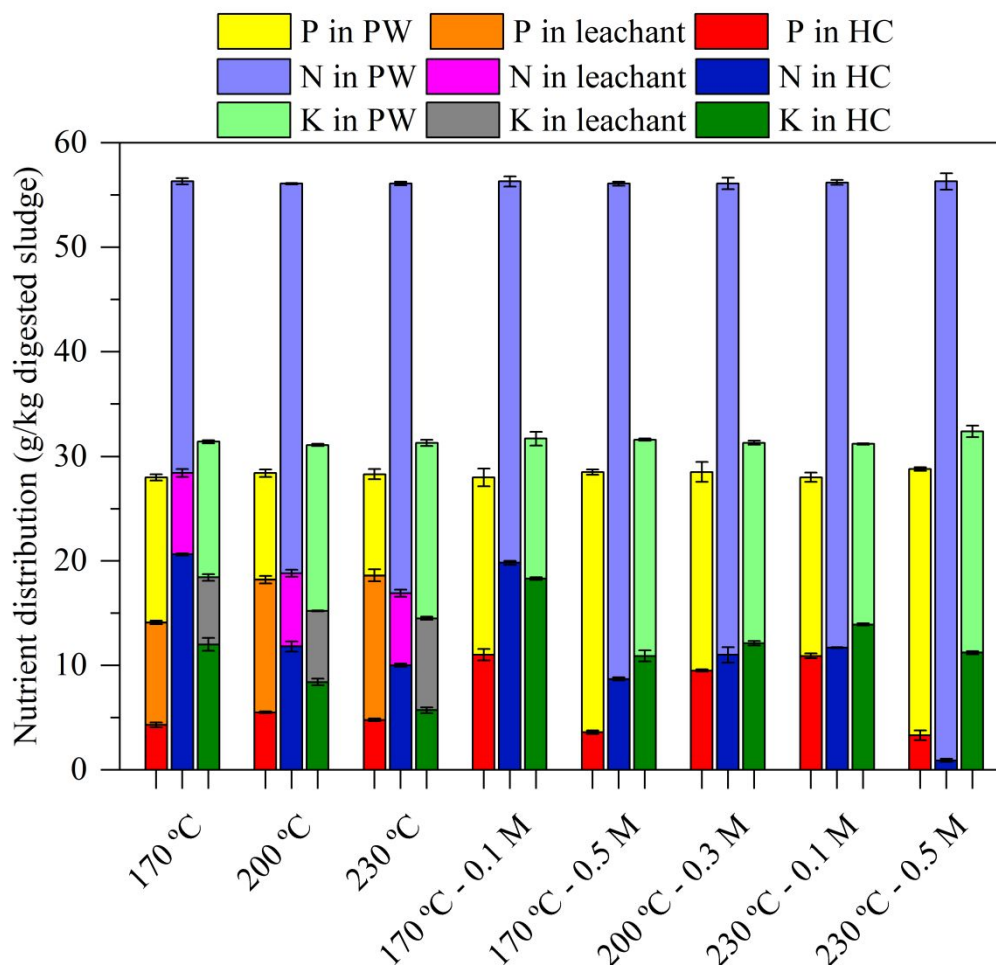
1
2
3 427 solubilized elements was reached. This fact was also observed by Ekpo et al. (2015)¹⁵ who
4
5 428 reported a partial K solubilization (60% of the K of digested sewage sludge) due to the
6
7 429 saturation of the process water with the large amount of elements in the feedstock and the
8
9 430 retention of some salts within the solid product formed during HTT. Alhnidi et al. (2022)⁵⁵
10
11 431 hydrothermally treated mimic anaerobically digestate at 180 – 260 °C for 3 h and observed
12
13 432 that most of K was solubilized in the process water but around 10 – 16 % remained sorbed in
14
15 433 the hydrochar structure.
16
17
18
19

20 434 **Strategies to promote nutrient release from digested sewage sludge**

21
22
23 435 **Fig. 4** shows a distribution of N₀, P₀ and K₀ (56.2 g/kg, 28.4 g/kg, and 32,7 g/kg dry
24
25 436 feedstock, respectively) along the acid-free HTT (process water plus leachant and HC-W) and
26
27 437 HCl-assisted HTT (process water plus hydrochar) (at 60 min reaction time). The fate of P for
28
29 438 all acid-free HTT processes appears to have been controlled by temperature. P was
30
31 439 predominantly retained in the hydrochar at the highest temperature (which corresponds to
32
33 440 18.6 g P/kg dry feedstock, equivalent to 65.5%, at 230 °C), likely due to the formation of
34
35 441 phosphate-metallic complexes that inhibited P solubilization. Diversely, an increase in
36
37 442 reaction temperature favored the release of N from the solids to the process water
38
39 443 (corresponding to the release of 39.2 g N/kg dry feedstock, equivalent to 69.8%, at 230 °C),
40
41 444 resulting from the hydrolysis and deamination of organic N. Similarly, K release to the
42
43 445 process water was also controlled by temperature (corresponding to the release of 16.8 g/kg
44
45 446 dry feedstock, equivalent to 51.4%, at 230 °C). The hydrochar washing with 0.5 M HCl is
46
47 447 more effective for nutrient release, especially P, from HC230, and promoted additional release
48
49 448 of P (corresponding to 13.8 g P/kg dry feedstock), N (equivalent to 7.0 g N/kg dry feedstock)
50
51 449 and K (equal to 8.8 g K/kg dry feedstock) to the leachant. Considering the nutrient release
52
53 450 both in the leachant and in the amount of nutrients solubilized directly in the process water,
54
55 451 the best operating condition was found at 230 °C, achieving a release of 83%, 82% and 78%
56
57
58
59
60

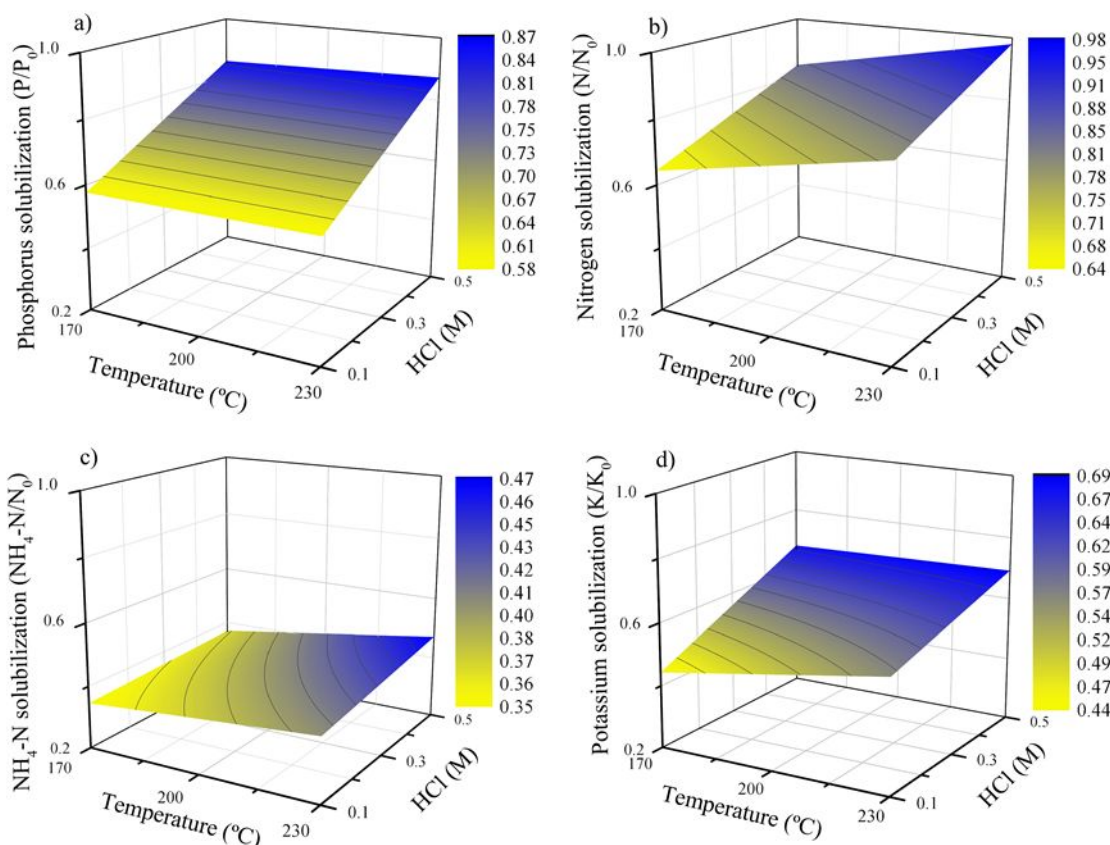
1
2
3 452 of P (as $\text{PO}_4\text{-P}$), N and K, respectively, from the raw digested sewage sludge thermally
4
5 453 treated.

6
7
8 454 In the case of HCl-assisted HTT, temperature showed a significant effect on nutrient release
9
10 455 to the process water regardless of HCl concentration. The highest HCl concentration (0.5 M)
11
12 456 favored N, P and K leaching, being this variable more significant in the case of N. Comparing
13
14 457 these results with those of acid-free HTT combined with hydrochar washing, the direct
15
16 458 nutrient release to the process water (using 0.5 M HCl) achieved the highest solubilization of
17
18 459 N and P (20 and 10% higher, respectively) than those obtained with combined route. In the
19
20 460 case of K, the best option to maximize its solubilization may be combining acid-free HTT and
21
22 461 acid washing of the hydrochar. However, considering the importance of nutrients for
23
24 462 fertilization purposes, P and N (as $\text{NH}_4\text{-N}$) recovery is more attractive. For this reason, HCl-
25
26 463 assisted HTT is considered a better option than acid-free HTT combined with hydrochar
27
28 464 washing for releasing nutrients directly in liquid phase and, therefore, amenable to in-depth
29
30 465 analysis.
31
32
33
34
35
36
37
38
39
40
41
42
43
44
45
46
47
48
49
50
51
52
53
54
55
56
57
58
59
60



466
 467 **Fig. 4.** Distribution of nutrients (P, N and K) in acid-free HTT (washed hydrochar, leachant
 468 and process water) and HCl-assisted HTT (hydrochar and process water) of digested sewage
 469 sludge.

470 A three-dimensional response surface study was conducted to evaluate the importance of
 471 operating conditions (temperature and HCl concentration) in maximizing nutrient release
 472 (**Fig. 5**). The third variable that could affect nutrient release is the reaction time, but as
 473 previously shown, the acidic medium allows obtaining the maximum nutrient concentration at
 474 60 min reaction time, thus this was the time selected to carry out this analysis. **Table 2**
 475 contains the equations of the factorial design that determine the solubilization of P (**Eq. 5**), N
 476 (**Eq. 6**), $\text{NH}_4\text{-N}$ (**Eq. 7**), and K (**Eq. 8**), as a function of temperature ($^{\circ}\text{C}$) and HCl
 477 concentration (M). Fitting of experimental data showed statistical significance ($p < 0.05$ and
 478 $R^2 > 99.5\%$).



479

480 **Fig. 5.** Response surface of phosphorus (a), nitrogen (b) $\text{NH}_4\text{-N}$ (c), and potassium (d)
 481 solubilization in process water of HCl-assisted HTT after 60 min reaction time.

482 **Table 2.** Describing equations of normalized P, N, $\text{NH}_4\text{-N}$, and K solubilization in HCl-
 483 assisted HTT as a function of temperature (T , °C) and HCl concentration (C , M) at 60 min
 484 reaction time.

Equation	R^2 (%)	Eq.
$P/P_o = 0.5134 - 0.000035 \cdot T + 0.56 \cdot C + 0.00076 \cdot T \cdot C$	99.73	(5)
$N/N_o = 0.002392 \cdot T + 0.4981 \cdot C - 0.000067 \cdot T \cdot C + 0.1888$	99.98	(6)
$\text{NH}_4 - \text{N}/N_o = 0.000749 \cdot T - 0.2715 \cdot C + 0.001929 \cdot T \cdot C + 0.199$	99.56	(7)
$K/K_o = 0.002399 \cdot T + 1.305 \cdot C - 0.004254 \cdot T \cdot C - 0.02268$	99.61	(8)

485 As can be seen in **Fig. 5**, the surfaces are plain, and it do not present any curvature because
 486 the factorial design generates a first-order equation since only two factors (temperature and
 487 HCl concentration) were considered. In **Fig. 5b**, the coupled effect between temperature and
 488 HCl addition mainly influenced N release, obtaining a maximum value of 98% at the most

1
2
3 489 severe HTT conditions (230 °C and 0.5 M HCl). Maximum N release as NH₄-N (47%) was
4
5 490 achieved under these conditions (**Fig. 5c**). Increasing the HCl concentration to 0.5 M was also
6
7 491 crucial in enhancing leaching of P as PO₄-P (≈ 87%) and K (≈ 69%) to the process water (**Fig.**
8
9 492 **5a** and **5d**, respectively), with the reaction temperature used not being decisive. From these
10
11 493 premises, HCl-assisted HTT of digested sewage sludge appears to be a promising alternative
12
13 494 to release N (as NH₄-N), P (as PO₄-P) and K in the process water in a single step. This
14
15 495 alternative treatment allows the recovery of nutrients with a higher yield to those obtained by
16
17 496 Ekpo et al. (2015)¹⁵ by acid-free HTT of digested sewage sludge at 170 and 250 °C for 60
18
19 497 min, and comparable, in the case of P, to those reported by Zhao et al. (2018)⁵⁶, who valorized
20
21 498 a digested farm sludge by HTT at 190 °C and then washing of the hydrochar with 1.5 M
22
23 499 H₂SO₄.

24
25
26 500 The nutrient-enriched liquid phases (PW230-0.5 or combined PW230 and L-230) could be
27
28 501 pH-adjusted for direct use as liquid fertilizer²³. However, this liquid stream would be
29
30 502 susceptible of containing high amount in organic compounds whose effect on plant growth
31
32 503 should be evaluated by fertilization analysis. Celletti et al. (2021)²⁴ studied the phytotoxic
33
34 504 effect of process water derived from HTT of swine manure used for hydroponic growth of
35
36 505 maize. They observed that process water rich in potentially phytotoxic substances (mainly
37
38 506 Na) and with a very alkaline pH reduced nutrient bioavailability and thus led to growth arrest.
39
40 507 However, they indicated that diluted process water with low levels of phytotoxins and
41
42 508 adequate content of essential nutrients could be adequate for appropriate germination and
43
44 509 growth of plants. Alternatively, nutrient recovery via chemical precipitation of struvite could
45
46 510 appear as an interesting option. This might be a crucial point to make the products profitable
47
48 511 in future for agricultural applications¹². This method allows obtaining a mineral rich in P and
49
50 512 NH₄-N, of growing interest due to the increasing scarcity of P. The recovery of K as KNO₃
51
52 513 could be possible by adding tartaric acid at controlled pH⁵⁷ or as potassium struvite
53
54
55
56
57
58
59
60

1
2
3 514 (MgKPO₄) from a liquid source with higher K content than NH₄-N⁵⁸. In this way, the process
4
5 515 water obtained under optimum conditions for nutrient solubilization (PW230-0.5) and that
6
7 516 liquid phase corresponding to mixed PW230 plus L-230, were subjected to struvite
8
9 517 precipitation to compare their characteristics. PW230-0.5 stands out for its PO₄-P (3.1 g/L),
10
11 518 NH₄-N (3.2 g/L), and Mg (0.5 g/L) concentration, essentials for struvite precipitation.
12
13 519 However, both PW230 (containing 1.0 g PO₄-P/L, and 2.3 g NH₄-N/L) and L-230 (containing
14
15 520 2.4 g PO₄-P/L, and 0.4 g NH₄-N/L) require mixing to achieve adequate nutrient concentration
16
17 521 for struvite precipitation. **Fig. 6** shows the mineral and heavy metals content and diffraction
18
19 522 patterns of solid precipitates (ST230-A and ST230-L), respectively. The structure of ST230-A
20
21 523 presented clear crystalline peaks (**Fig. 6b**) similar to pure struvite (**Fig. 6a**) and remarkable N
22
23 524 (93.3 g/kg), PO₄-P (164.4 g/kg), and Mg (123.8 g/kg) contents. On the contrary, ST230-L
24
25 525 (**Fig. 6d**) did not show struvite peaks, but corresponded to NaCl (**Fig. 6c**), due to the
26
27 526 neutralization of hydrochloric acid from the leachant during the precipitation step, and
28
29 527 presented lower N (45.9 g/kg), PO₄-P (55.8 g/kg), and Mg (43.6 g/kg) contents than ST230-A.
30
31 528 In addition, a higher Si concentration was observed in ST230-L (362.7 g Si/kg) with respect
32
33 529 to ST230-A (91.2 g Si/kg). This fact is correlated with the ash content of the hydrochars
34
35 530 shown in **Table 1**, showing HC230-0.5 a higher ash content than HC230-W. Then, a lower
36
37 531 inorganic concentration was released to process water during HCl-assisted HTT in
38
39 532 comparison to those inorganics transferred to leachant after hydrochar washing, which may
40
41 533 precipitate together with struvite. The higher retention of inorganic elements in the hydrochar
42
43 534 during HCl-assisted HTT, which did not precipitate together with struvite, contributed to
44
45 535 improve final product specifications. In this way, only ST230-A considered as a potential
46
47 536 struvite. The ST230-A recovery yield was 223.2 g struvite per kg dry digested sewage sludge,
48
49 537 and the N/P/K content of the struvite was 9.3/37.5/0.7, following the same considerations as
50
51 538 for an industrial fertilizer (the N/P/K of the commercial struvite was 10.1/51.5/0). In addition,
52
53
54
55
56
57
58
59
60

1
2
3 539 the struvite contained 1.9% total organic C and heavy metals content was negligible.
4
5 540 According to metal composition, some impurities including Cl^- containing compounds (such
6
7 541 as NaCl or MgCl_2) could be present, whose excess is considered harmful to agriculture
8
9 542 because of its toxic effects and its antagonistic interaction with NO_3^- , which impairs NO_3^-
10
11 543 nutrition and reduces crop yield⁵⁹. However, the use of struvite-like precipitate as a fertilizer
12
13 544 is potentially suitable according to Regulation (EU) 2019/1009 on fertilizing products³⁴.
14
15
16
17 545 The integration of HTT with nutrient recovery for digested sewage sludge management can
18
19 546 be a potential source of value-added products. Following the methodology reported by
20
21 547 Mannarino et al. (2022)⁶⁰ for the estimation of the energy input of a similar process using
22
23 548 food waste as feedstock, the cost of the process at the optimum operating conditions to obtain
24
25 549 the highest nutrient solubilization (230 °C and 1h, considering the HCl requirements
26
27 550 negligible) is estimated to be approximately 13.7 € per tonne of treated digested sewage
28
29 551 sludge. This economic approximation takes into account the electricity input of the HTT
30
31 552 reactor (3,800 to 5,200 kWh per tonne of dry raw material), together with additional units
32
33 553 such as slurry separation, drying and pelletizing of the hydrochar. Furthermore, it considers
34
35 554 both the electricity price for non-household customers⁶¹ and the output associated to the
36
37 555 energy content of the hydrochar²¹. Moreover, the energy valorization of process water by
38
39 556 anaerobic digestion for obtaining biogas⁶², or by dark fermentation⁶³ or aqueous phase
40
41 557 reforming⁶⁴ to produce hydrogen add outputs to the process. According to Medina-Martos et
42
43 558 al. (2020)⁶⁵ energy input for HTT of sewage sludge at 210 °C for 1 h coupled to an anaerobic
44
45 559 digestion stage resulted in an energy cost around 10 € per tonne of treated sewage sludge,
46
47 560 which is in accordance with the cost estimation of our process. This value is significantly
48
49 561 lower than other alternatives such as anaerobic fermentation plus P releasing from dewatered
50
51 562 anaerobic sludge by sequential extraction with H_2SO_4 acidified water and sulphur-reducing
52
53 563 bacteria, which is around 110 € per treated tonne of sludge⁶⁶, and even the HCl plus H_2O_2 -
54
55
56
57
58
59
60

1
2
3 564 assisted hydrothermal carbonization of digestate (around 50 € per tonne of digestate) with
4
5 565 subsequent struvite crystallization from the process water²⁵. Regarding struvite precipitation,
6
7 566 the cost of the required reagents (MgCl₂ and NaOH) results in about 1.6 € per tonne of
8
9 567 digested sewage sludge^{25,27,67}, which is in the cost range of chemicals for struvite precipitation
10
11 568 using biomass waste (1 – 2 € per tonne of biomass waste^{25,68–70}). This prediction of the cost
12
13 569 could be improved in a continuous HTT setup, where energy recovery can be optimized by
14
15 570 integrating the streams involved in the process, which significantly saves the required energy
16
17 571 inputs^{65,71}.
18
19
20
21
22
23
24
25
26
27
28
29
30
31
32
33
34
35
36
37
38
39
40
41
42
43
44
45
46
47
48
49
50
51
52
53
54
55
56
57
58
59
60

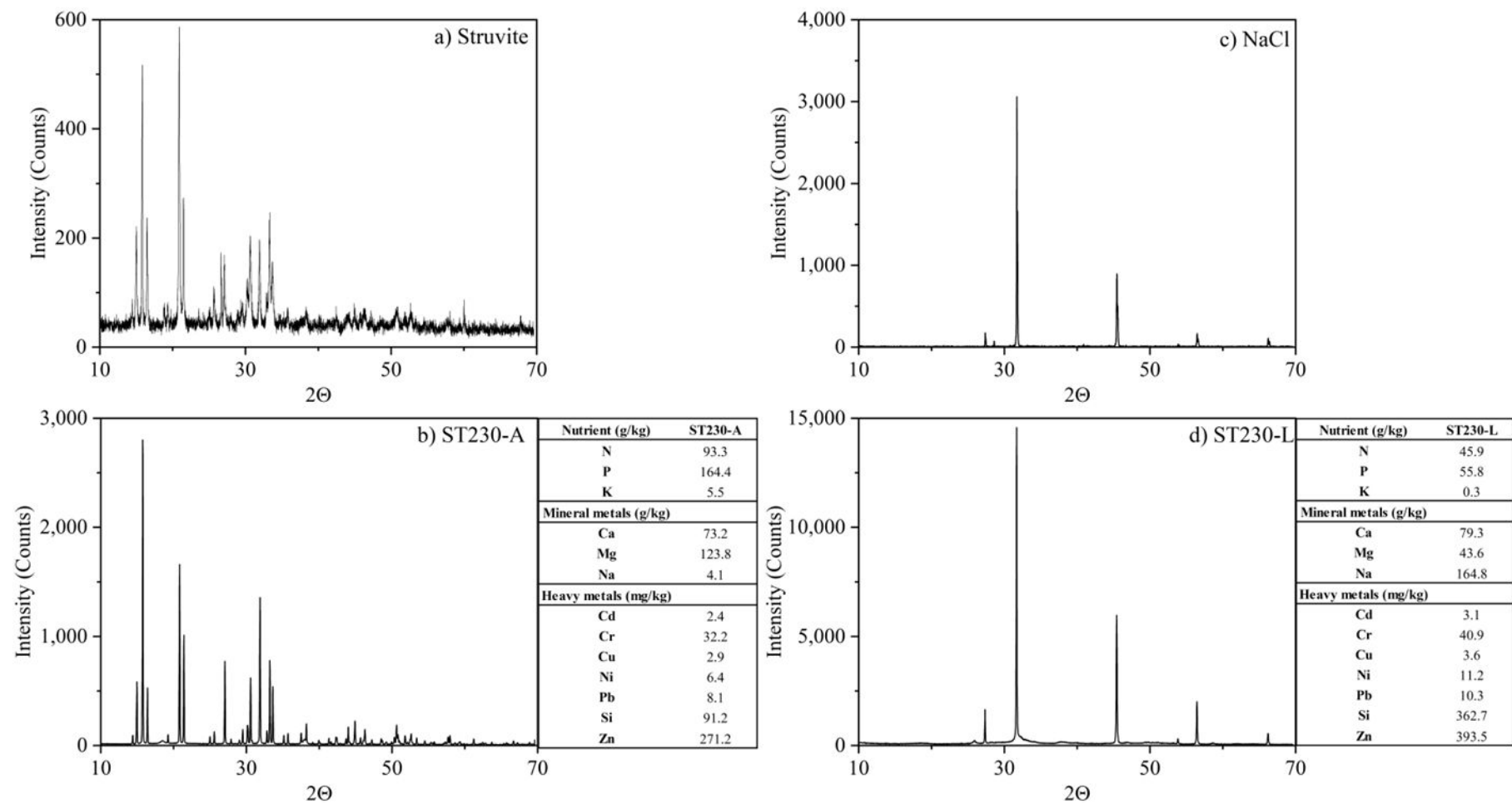


Fig. 6. X-ray diffractogram and nutrient content of a) commercial struvite, b) ST230-A, c) commercial NaCl, and d) ST230-L.

575 **Conclusions**

576 Two nutrient release strategies based on HTT of digested sewage sludge were studied in this
577 work. The HCl-assisted HTT showed the best performance on nutrient solubilization directly
578 into process water, achieving under optimum conditions (230 °C, 60 min, and 0.5 M HCl), up
579 to 87% of P (as PO₄-P), 98% of N (as organic N and 47% of NH₄-N) and 69% of K release.
580 The combined strategy based on acid-free HTT (nutrient solubilization into process water) and
581 hydrochar acid washing (nutrient concentrated in a leachant) showed lower nutrient release
582 yield (80 – 82% P, 60 – 82% N, and 59 – 78% K). Only using the best HCl-assisted HTT
583 conditions yielded a solid with struvite-like characteristics through chemical precipitation from
584 the process water.

585 **Supporting information**

586 Heavy metal content in digested sewage sludge and hydrochar according to Regulation (EU)
587 2019/1009.

588 **Author information**

589 **Corresponding author**

590 **Andres Sarrion** - Department of Chemical Engineering, Faculty of Sciences, Universidad
591 Autonoma de Madrid, Campus de Cantoblanco, 28049, Madrid, Spain
592 <https://orcid.org/0000-0002-5301-7653>; Email: andres.sarrion@uam.es

593 **Authors**

594 **Angeles de la Rubia** - Department of Chemical Engineering, Faculty of Sciences,
595 Universidad Autonoma de Madrid, Campus de Cantoblanco, 28049, Madrid, Spain

596 **Nicole D. Berge** - Civil and Environmental Engineering Dept., University of South Carolina,
597 Columbia, 300 Main St., 29201, South Carolina, United States

1
2
3 598 **Angel F. Mohedano** - Department of Chemical Engineering, Faculty of Sciences,
4
5 599 Universidad Autonoma de Madrid, Campus de Cantoblanco, 28049, Madrid, Spain
6
7 600 **Elena Diaz** - Department of Chemical Engineering, Faculty of Sciences, Universidad
8
9 601 Autonoma de Madrid, Campus de Cantoblanco, 28049, Madrid, Spain
10
11

12 602 **Acknowledgements**

13
14
15 603 The authors greatly appreciate funding from Spanish MICINN (Project PID2019-108445RB-
16
17 604 I00; PDC2021-120755-I00) and the Madrid Regional Government (Project S2018/EMT-
18
19 605 4344). A. Sarrion wishes to thank the Spanish MICINN and ESF for a research grant (BES-
20
21 606 2017-081515).
22
23
24

25 607 **Data availability**

26
27
28 608 Data will be made available on request
29
30

31 609 **References**

- 32
33 610 (1) de La Rubia, M. A.; Villamil, J. A.; Mohedano, A. F. Anaerobic Digestion for Methane
34
35 611 and Hydrogen Production. *Wastewater Treatment Residues as Resources for*
36
37 612 *Biorefinery Products and Biofuels* **2020**, 67–83. [https://doi.org/10.1016/B978-0-12-](https://doi.org/10.1016/B978-0-12-816204-0.00004-7)
38
39 613 816204-0.00004-7.
40
41
42
43 614 (2) Merzari, F.; Langone, M.; Andreottola, G.; Fiori, L. Methane Production from Process
44
45 615 Water of Sewage Sludge Hydrothermal Carbonization. A Review. Valorising Sludge
46
47 616 through Hydrothermal Carbonization. *Crit Rev Environ Sci Technol* **2019**, 49 (11),
48
49 617 947–988. <https://doi.org/10.1080/10643389.2018.1561104>.
50
51
52
53 618 (3) Aragón-Briceño, C.; Ross, A. B.; Camargo-Valero, M. A. Evaluation and Comparison
54
55 619 of Product Yields and Bio-Methane Potential in Sewage Digestate Following
56
57 620 Hydrothermal Treatment. *Appl Energy* **2017**, 208 (August), 1357–1369.
58
59 621 <https://doi.org/10.1016/j.apenergy.2017.09.019>.

- 1
2
3 622 (4) Marin-Batista, J. D.; Mohedano, A. F.; Rodríguez, J. J.; de la Rubia, M. A. Energy and
4
5 623 Phosphorous Recovery through Hydrothermal Carbonization of Digested Sewage
6
7 624 Sludge. *Waste Management* **2020**, *105*, 566–574.
8
9
10 625 <https://doi.org/10.1016/j.wasman.2020.03.004>.
11
12
13 626 (5) Ekpo, U.; Ross, A. B.; Camargo-Valero, M. A.; Fletcher, L. A. Influence of PH on
14
15 627 Hydrothermal Treatment of Swine Manure: Impact on Extraction of Nitrogen and
16
17 628 Phosphorus in Process Water. *Bioresour Technol* **2016**, *214*, 637–644.
18
19
20 629 <https://doi.org/10.1016/J.BIORTECH.2016.05.012>.
21
22
23 630 (6) Szögi, A. A.; Vanotti, M. B.; Hunt, P. G. Phosphorus Recovery from Pig Manure
24
25 631 Solids Prior to Land Application. *J Environ Manage* **2015**, *157* (March 2018), 1–7.
26
27 632 <https://doi.org/10.1016/j.jenvman.2015.04.010>.
28
29
30 633 (7) Qaramaleki, S. V.; Villamil, J. A.; Mohedano, A. F.; Coronella, C. J. Factors Affecting
31
32 634 Solubilization of Phosphorus and Nitrogen through Hydrothermal Carbonization of
33
34 635 Animal Manure. *ACS Sustain Chem Eng* **2020**, *8* (33), 12462–12470.
35
36
37 636 <https://doi.org/10.1021/acssuschemeng.0c03268>.
38
39
40 637 (8) Idowu, I.; Li, L.; Flora, J. R. V.; Pellechia, P. J.; Darko, S. A.; Ro, K. S.; Berge, N. D.
41
42 638 Hydrothermal Carbonization of Food Waste for Nutrient Recovery and Reuse. *Waste*
43
44 639 *Management* **2017**, *105*, 566–574. <https://doi.org/10.1016/j.wasman.2017.08.051>.
45
46
47 640 (9) Akarsu, K.; Duman, G.; Yilmazer, A.; Keskin, T.; Azbar, N.; Yanik, J. Sustainable
48
49 641 Valorization of Food Wastes into Solid Fuel by Hydrothermal Carbonization.
50
51 642 *Bioresour Technol* **2019**, *292* (July), 121959.
52
53 643 <https://doi.org/10.1016/j.biortech.2019.121959>.
54
55
56
57
58
59
60

- 1
2
3 644 (10) Sarrion, A.; Diaz, E.; de la Rubia, M. A.; Mohedano, A. F. Fate of Nutrients during
4
5 645 Hydrothermal Treatment of Food Waste. *Bioresour Technol* **2021**, *342*, 125954.
6
7 646 <https://doi.org/10.1016/J.BIORTECH.2021.125954>.
8
9
10 647 (11) Alexandratos, N.; Bruinsma, J. WORLD AGRICULTURE TOWARDS 2030 / 2050
11
12 648 The 2012 Revision. 2012, p 146.
13
14
15 649 (12) Aragón-Briceño, C. I.; Pozarlik, A. K.; Bramer, E. A.; Niedzwiecki, L.; Pawlak-
16
17 650 Kruczek, H.; Brem, G. Hydrothermal Carbonization of Wet Biomass from Nitrogen
18
19 651 and Phosphorus Approach: A Review. *Renew Energy* **2021**, *171*, 401–415.
20
21 652 <https://doi.org/10.1016/j.renene.2021.02.109>.
22
23
24
25 653 (13) Gerner, G.; Meyer, L.; Wanner, R.; Keller, T. Sewage Sludge Treatment by
26
27 654 Hydrothermal Carbonization: Fuel Production. *Energies (Basel)* **2021**, *14*, 2697, 1–12.
28
29
30 655 (14) He, M.; Zhu, X.; Dutta, S.; Khanal, S. K.; Lee, K. T.; Masek, O.; Tsang, D. C. W.
31
32 656 Catalytic Co-Hydrothermal Carbonization of Food Waste Digestate and Yard Waste
33
34 657 for Energy Application and Nutrient Recovery. *Bioresour Technol* **2022**, *344*.
35
36 658 <https://doi.org/10.1016/J.BIORTECH.2021.126395>.
37
38
39
40 659 (15) Ekpo, U.; Ross, A. B.; Camargo-Valero, M. A.; Williams, P. T. A Comparison of
41
42 660 Product Yields and Inorganic Content in Process Streams Following Thermal
43
44 661 Hydrolysis and Hydrothermal Processing of Microalgae, Manure and Digestate.
45
46 662 *Bioresour Technol* **2015**, *200*, 951–960. <https://doi.org/10.1016/j.biortech.2015.11.018>.
47
48
49
50 663 (16) Li, L.; Flora, J. R. V.; Berge, N. D. Predictions of Energy Recovery from Hydrochar
51
52 664 Generated from the Hydrothermal Carbonization of Organic Wastes. *Renew Energy*
53
54 665 **2020**, *145*, 1883–1889. <https://doi.org/10.1016/j.renene.2019.07.103>.
55
56
57
58
59
60

- 1
2
3 666 (17) Wang, X.; Wei-Chung Chang, V.; Li, Z.; Song, Y.; Li, C.; Wang, Y. Co-Pyrolysis of
4
5 667 Sewage Sludge and Food Waste Digestate to Synergistically Improve Biochar
6
7 668 Characteristics and Heavy Metals Immobilization. *Waste Management* **2022**, *141*, 231–
8
9 669 239. <https://doi.org/10.1016/J.WASMAN.2022.02.001>.
10
11
12
13 670 (18) Marchese, M.; Chesta, S.; Santarelli, M.; Lanzini, A. Techno-Economic Feasibility of a
14
15 671 Biomass-to-X Plant: Fischer-Tropsch Wax Synthesis from Digestate Gasification.
16
17 672 *Energy* **2021**, *228*, 120581. <https://doi.org/10.1016/J.ENERGY.2021.120581>.
18
19
20
21 673 (19) Dziejczak, K.; Łapczyńska-kordon, B.; Jurczyk, M.; Arczewska, M.; Wróbel, M.;
22
23 674 Jewiarz, M.; Mudryk, K.; Pająk, T. Solid Digestate—Physicochemical and Thermal
24
25 675 Study. *Energies* **2021**, *Vol. 14*, Page 7224 **2021**, *14* (21), 7224.
26
27 676 <https://doi.org/10.3390/EN14217224>.
28
29
30
31 677 (20) Heidari, M.; Dutta, A.; Acharya, B.; Mahmud, S. A Review of the Current Knowledge
32
33 678 and Challenges of Hydrothermal Carbonization for Biomass Conversion. *Journal of the*
34
35 679 *Energy Institute* **2019**, *92* (6), 1779–1799. <https://doi.org/10.1016/J.JOEL.2018.12.003>.
36
37
38 680 (21) Ipiates, R. P.; de la Rubia, M. A.; Diaz, E.; Mohedano, A. F.; Rodriguez, J. J.
39
40 681 Integration of Hydrothermal Carbonization and Anaerobic Digestion for Energy
41
42 682 Recovery of Biomass Waste: An Overview. *Energy & Fuels* **2021**, *35* (21), 17032–
43
44 683 17050. <https://doi.org/10.1021/ACS.ENERGYFUELS.1C01681>.
45
46
47
48 684 (22) Dai, L.; Yang, B.; Li, H.; Tan, F.; Zhu, N.; Zhu, Q.; He, M.; Ran, Y.; Hu, G. A
49
50 685 Synergistic Combination of Nutrient Reclamation from Manure and Resultant
51
52 686 Hydrochar Upgradation by Acid-Supported Hydrothermal Carbonization. *Bioresour*
53
54 687 *Technol* **2017**, *243*, 860–866. <https://doi.org/10.1016/j.biortech.2017.07.016>.
55
56
57
58
59
60

- 1
2
3 688 (23) De Mena Pardo, B.; Doyle, L.; Renz, M.; Salimbeni, A. *Industrial Scale Hydrothermal*
4
5 689 *Carbonization: New Applications for Wet Biomass Waste*; Ttz Bremerhaven:
6
7 690 Bremerhaven, Germany, 2016.
- 9
10 691 (24) Celletti, S.; Lanz, M.; Bergamo, A.; Benedetti, V.; Basso, D.; Baratieri, M.; Cesco, S.;
11
12 692 Mimmo, T. Evaluating the Aqueous Phase From Hydrothermal Carbonization of Cow
13
14 693 Manure Digestate as Possible Fertilizer Solution for Plant Growth. *Front Plant Sci*
15
16 694 **2021**, *12*, 1317. <https://doi.org/10.3389/FPLS.2021.687434>.
- 17
18 695 (25) Zhang, T.; He, X.; Deng, Y.; Tsang, D. C. W.; Jiang, R.; Becker, G. C.; Kruse, A.
19
20 696 Phosphorus Recovered from Digestate by Hydrothermal Processes with Struvite
21
22 697 Crystallization and Its Potential as a Fertilizer. *Science of The Total Environment* **2020**,
23
24 698 *698*, 134240. <https://doi.org/10.1016/J.SCITOTENV.2019.134240>.
- 25
26 699 (26) Talboys, P. J.; Heppell, J.; Roose, T.; Healey, J. R.; Jones, D. L.; Withers, P. J. A.
27
28 700 Struvite: A Slow-Release Fertiliser for Sustainable Phosphorus Management? *Plant*
29
30 701 *Soil* **2016**, *401* (1–2), 109–123. <https://doi.org/10.1007/S11104-015-2747-3>.
- 31
32 702 (27) Becker, G. C.; Wüst, D.; Köhler, H.; Lautenbach, A.; Kruse, A. Novel Approach of
33
34 703 Phosphate-Reclamation as Struvite from Sewage Sludge by Utilising Hydrothermal
35
36 704 Carbonization. *J Environ Manage* **2019**, *238* (August 2018), 119–125.
37
38 705 <https://doi.org/10.1016/j.jenvman.2019.02.121>.
- 39
40 706 (28) Zheng, X.; Ye, Y.; Jiang, Z.; Ying, Z.; Ji, S.; Chen, W.; Wang, B.; Dou, B. Enhanced
41
42 707 Transformation of Phosphorus (P) in Sewage Sludge to Hydroxyapatite via
43
44 708 Hydrothermal Carbonization and Calcium-Based Additive. *Sci Total Environ* **2020**,
45
46 709 *738*. <https://doi.org/10.1016/J.SCITOTENV.2020.139786>.
- 47
48
49
50
51
52
53
54
55
56
57
58
59
60

- 1
2
3 710 (29) Pastor, L.; Mangin, D.; Barat, R.; Seco, A. A Pilot-Scale Study of Struvite Precipitation
4
5 711 in a Stirred Tank Reactor: Conditions Influencing the Process. *Bioresour Technol*
6
7 712 **2008**, *99* (14), 6285–6291. <https://doi.org/10.1016/J.BIORTECH.2007.12.003>.
8
9
10 713 (30) Channiwala, S. A.; Parikh, P. P. A Unified Correlation for Estimating HHV of Solid,
11
12 714 Liquid and Gaseous Fuels. *Fuel* **2002**, *81* (8), 1051–1063.
13
14 715 [https://doi.org/10.1016/S0016-2361\(01\)00131-4](https://doi.org/10.1016/S0016-2361(01)00131-4).
15
16
17
18 716 (31) Pardo, P.; Rauret, G.; López-Sánchez, J. F. Shortened Screening Method for
19
20 717 Phosphorus Fractionation in Sediments: A Complementary Approach to the Standards,
21
22 718 Measurements and Testing Harmonised Protocol. *Anal Chim Acta* **2004**, *508* (2), 201–
23
24 719 206. <https://doi.org/10.1016/j.aca.2003.11.005>.
25
26
27
28 720 (32) American Public Health Association; Eaton, A. D.; Clesceri, L. S.; Rice, E. W.
29
30 721 *Standard Methods for Examination of Water and Wastewater*, 21st ed.; Washington
31
32 722 DC: APHA press, Ed.; American Public Health Association: Washington DC, 2005.
33
34
35
36 723 (33) Dhawan, H.; Sharma, D. K. Advances in the Chemical Leaching (Inorgano-Leaching),
37
38 724 Bio-Leaching and Desulphurisation of Coals. *Int J Coal Sci Technol* **2019**, *6* (2), 169–
39
40 725 183. <https://doi.org/10.1007/S40789-019-0253-6>.
41
42
43 726 (34) European Commission. Regulation EU 2019/1009. *Official Journal of the European*
44
45 727 *Union* **2022**, *129*, 1–125.
46
47
48 728 (35) George, C.; Wagner, M.; Kücke, M.; Rillig, M. C. Divergent Consequences of
49
50 729 Hydrochar in the Plant–Soil System: Arbuscular Mycorrhiza, Nodulation, Plant
51
52 730 Growth and Soil Aggregation Effects. *Applied Soil Ecology* **2012**, *59*, 68–72.
53
54 731 <https://doi.org/https://doi.org/10.1016/j.apsoil.2012.02.021>.
55
56
57
58
59
60

- 1
2
3 732 (36) de Jager, M.; Giani, L. An Investigation of the Effects of Hydrochar Application Rate
4
5 733 on Soil Amelioration and Plant Growth in Three Diverse Soils. *Biochar* **2021**, *3* (3),
6
7 734 349–365. <https://doi.org/10.1007/S42773-021-00089-Z>.
- 9
10 735 (37) Eskandari, S.; Mohammadi, A.; Sandberg, M.; Eckstein, R. L.; Hedberg, K.;
11
12 736 Granström, K. Hydrochar-Amended Substrates for Production of Containerized Pine
13
14 737 Tree Seedlings under Different Fertilization Regimes. *Agronomy* **2019**, *Vol. 9*, Page
15
16 738 *350* **2019**, *9* (7), 350. <https://doi.org/10.3390/AGRONOMY9070350>.
- 17
18 739 (38) Shi, Y.; Luo, G.; Rao, Y.; Chen, H.; Zhang, S. Hydrothermal Conversion of Dewatered
19
20 740 Sewage Sludge: Focusing on the Transformation Mechanism and Recovery of
21
22 741 Phosphorus. *Chemosphere* **2019**, *228*, 619–628.
23
24 742 <https://doi.org/10.1016/j.chemosphere.2019.04.109>.
- 25
26 743 (39) Huang, R.; Tang, Y. Evolution of Phosphorus Complexation and Mineralogy during
27
28 744 (Hydro)Thermal Treatments of Activated and Anaerobically Digested Sludge: Insights
29
30 745 from Sequential Extraction and P K-Edge XANES. *Water Res* **2016**, *100*, 439–447.
31
32 746 <https://doi.org/10.1016/j.watres.2016.05.029>.
- 33
34 747 (40) Zheng, X.; Zheng, X.; Jiang, Z.; Ying, Z.; Ying, Z.; Ye, Y.; Chen, W.; Wang, B.;
35
36 748 Wang, B.; Dou, B.; Dou, B. Migration and Transformation of Phosphorus during
37
38 749 Hydrothermal Carbonization of Sewage Sludge: Focusing on the Role of PH and
39
40 750 Calcium Additive and the Transformation Mechanism. *ACS Sustain Chem Eng* **2020**, *8*
41
42 751 (21), 7806–7814. <https://doi.org/10.1021/acssuschemeng.0c00031>.
- 43
44 752 (41) Huang, R.; Fang, C.; Zhang, B.; Tang, Y. Transformations of Phosphorus Speciation
45
46 753 during (Hydro)Thermal Treatments of Animal Manures. *Environ Sci Technol* **2018**, *52*
47
48 754 (5), 3016–3026. <https://doi.org/10.1021/acs.est.7b05203>.
- 49
50
51
52
53
54
55
56
57
58
59
60

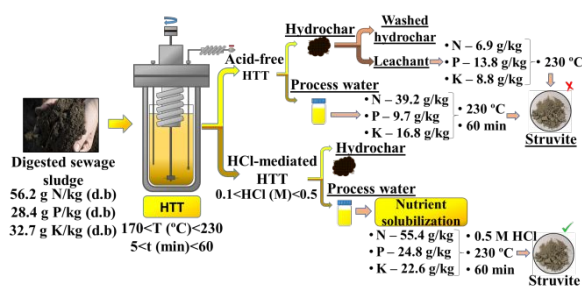
- 1
2
3 755 (42) Sarrion, A.; de la Rubia, A.; Coronella, C.; Mohedano, A. F.; Diaz, E. Acid-Mediated
4
5 756 Hydrothermal Treatment of Sewage Sludge for Nutrient Recovery. *Science of The*
6
7 757 *Total Environment* **2022**, 156494.
8
9
10 758 <https://doi.org/10.1016/J.SCITOTENV.2022.156494>.
11
12
13 759 (43) Huang, R.; Tang, Y. Speciation Dynamics of Phosphorus during (Hydro)Thermal
14
15 760 Treatments of Sewage Sludge. *Environ Sci Technol* **2015**, 49 (24), 14466–14474.
16
17 761 <https://doi.org/10.1021/acs.est.5b04140>.
18
19
20 762 (44) Sengupta, S.; Nawaz, T.; Beaudry, J. Nitrogen and Phosphorus Recovery from
21
22 763 Wastewater. *Curr Pollut Rep* **2015**, 1 (3), 155–166. <https://doi.org/10.1007/s40726->
23
24 764 015-0013-1.
25
26
27
28 765 (45) Rodriguez Correa, C.; Bernardo, M.; Ribeiro, R. P. P. L.; Esteves, I. A. A. C.; Kruse,
29
30 766 A. Evaluation of Hydrothermal Carbonization as a Preliminary Step for the Production
31
32 767 of Functional Materials from Biogas Digestate. *J Anal Appl Pyrolysis* **2017**, 124, 461–
33
34 768 474. <https://doi.org/10.1016/j.jaap.2017.02.014>.
35
36
37
38 769 (46) Palacios, E.; Leret, P.; De La Mata, M. J.; Fernández, J. F.; De Aza, A. H.; Rodríguez,
39
40 770 M. A. Influence of the PH and Ageing Time on the Acid Aluminum Phosphate
41
42 771 Synthesized by Precipitation. *CrystEngComm* **2013**, 15 (17), 3359–3365.
43
44 772 <https://doi.org/10.1039/c3ce00011g>.
45
46
47
48 773 (47) Mekmene, O.; Quillard, S.; Rouillon, T.; Bouler, J. M.; Piot, M.; Gaucheron, F. Effects
49
50 774 of PH and Ca/P Molar Ratio on the Quantity and Crystalline Structure of Calcium
51
52 775 Phosphates Obtained from Aqueous Solutions. *Dairy Sci Technol* **2009**, 89 (3–4), 301–
53
54 776 316. <https://doi.org/10.1051/dst/2009019>.
55
56
57
58
59
60

- 1
2
3 777 (48) Kruse, A.; Koch, F.; Stelzl, K.; Wüst, D.; Zeller, M. Fate of Nitrogen during
4
5 778 Hydrothermal Carbonization. *Energy and Fuels* **2016**, *30* (10), 8037–8042.
6
7 779 <https://doi.org/10.1021/acs.energyfuels.6b01312>.
8
9
10 780 (49) Zhang, Y.; Jiang, Q.; Xie, W.; Wang, Y.; Kang, J. Effects of Temperature, Time and
11
12 781 Acidity of Hydrothermal Carbonization on the Hydrochar Properties and Nitrogen
13
14 782 Recovery from Corn Stover. *Biomass Bioenergy* **2019**, *122* (February), 175–182.
15
16 783 <https://doi.org/10.1016/j.biombioe.2019.01.035>.
17
18
19 784 (50) He, C.; Wang, K.; Yang, Y.; Amaniampong, P. N.; Wang, J. Y. Effective Nitrogen
20
21 785 Removal and Recovery from Dewatered Sewage Sludge Using a Novel Integrated
22
23 786 System of Accelerated Hydrothermal Deamination and Air Stripping. *Environ Sci*
24
25 787 *Technol* **2015**, *49* (11), 6872–6880. <https://doi.org/10.1021/acs.est.5b00652>.
26
27
28 788 (51) Xiao, H.; Zhai, Y.; Xie, J.; Wang, T.; Wang, B.; Li, S.; Li, C. Speciation and
29
30 789 Transformation of Nitrogen for Spirulina Hydrothermal Carbonization. *Bioresour*
31
32 790 *Technol* **2019**, *286*. <https://doi.org/10.1016/j.biortech.2019.121385>.
33
34
35 791 (52) Li, D. C.; Jiang, H. The Thermochemical Conversion of Non-Lignocellulosic Biomass
36
37 792 to Form Biochar: A Review on Characterizations and Mechanism Elucidation.
38
39 793 *Bioresource Technology*. Elsevier Ltd December 1, 2017, pp 57–68.
40
41 794 <https://doi.org/10.1016/j.biortech.2017.07.029>.
42
43
44 795 (53) Wang, T.; Zhai, Y.; Zhu, Y.; Peng, C.; Xu, B.; Wang, T.; Li, C.; Zeng, G. Influence of
45
46 796 Temperature on Nitrogen Fate during Hydrothermal Carbonization of Food Waste.
47
48 797 *Bioresour Technol* **2018**, *247*, 182–189. <https://doi.org/10.1016/j.biortech.2017.09.076>.
49
50
51 798 (54) Funke, A. Fate of Plant Available Nutrients during Hydrothermal Carbonization of
52
53 799 Digestate. *Chem Ing Tech* **2015**, *87* (12), 1713–1719.
54
55
56 800 <https://doi.org/10.1002/cite.201400182>.
57
58
59
60

- 1
2
3 801 (55) Alhnidi, M. J.; Wüst, D.; Funke, A.; Hang, L.; Kruse, A. Fate of Nitrogen, Phosphate,
4
5 802 and Potassium during Hydrothermal Carbonization and the Potential for Nutrient
6
7 803 Recovery. *ACS Sustain Chem Eng* **2020**, *8* (41), 15507–15516.
8
9
10 804 <https://doi.org/10.1021/ACSSUSCHEMENG.0C04229/ASSET/IMAGES/LARGE/SC>
11
12 805 [0C04229_0005.JPEG](https://doi.org/10.1021/ACSSUSCHEMENG.0C04229/ASSET/IMAGES/LARGE/SC).
13
14
15 806 (56) Zhao, X.; Becker, G. C.; Faweya, N.; Rodriguez Correa, C.; Yang, S.; Xie, X.; Kruse,
16
17 807 A. Fertilizer and Activated Carbon Production by Hydrothermal Carbonization of
18
19 808 Digestate. *Biomass Convers Biorefin* **2018**, *8*, 423–436.
20
21
22 809 <https://doi.org/10.1007/s13399-017-0291-5>.
23
24
25 810 (57) Khatri, I.; Garg, A. Potash Recovery from Synthetic Potassium Rich Wastewater and
26
27 811 Biomethanated Distillery Effluent Using Tartaric Acid as a Recyclable Precipitant.
28
29 812 *Environ Technol Innov* **2022**, *28*, 102841. <https://doi.org/10.1016/J.ETI.2022.102841>.
30
31
32 813 (58) Crossley, O. P.; Thorpe, R. B.; Lee, J. Phosphorus Recovery from Process Waste
33
34 814 Water Made by the Hydrothermal Carbonisation of Spent Coffee Grounds. *Bioresour*
35
36 815 *Technol* **2020**, *301*, 122664. <https://doi.org/10.1016/J.BIORTECH.2019.122664>.
37
38
39 816 (59) Rosales, M. A.; Franco-Navarro, J. D.; Peinado-Torrubia, P.; Díaz-Rueda, P.; Álvarez,
40
41 817 R.; Colmenero-Flores, J. M. Chloride Improves Nitrate Utilization and NUE in Plants.
42
43 818 *Front Plant Sci* **2020**, *11*, 442. <https://doi.org/10.3389/FPLS.2020.00442/BIBTEX>.
44
45
46 819 (60) Mannarino, G.; Sarrion, A.; Diaz, E.; Gori, R.; de la Rubia, M. A.; Mohedano, A. F.
47
48 820 Improved Energy Recovery from Food Waste through Hydrothermal Carbonization
49
50 821 and Anaerobic Digestion. *Waste Management* **2022**, *142*, 9–18.
51
52
53 822 <https://doi.org/10.1016/J.WASMAN.2022.02.003>.
54
55
56 823 (61) Eurostat. *Electricity prices for non-household consumers - S2, 2022*.
57
58 824 <https://ec.europa.eu/eurostat/statistics->
59
60

- 1
2
3 825 explained/index.php?title=Electricity_price_statistics#Electricity_prices_for_non-
4
5 826 household_consumers (accessed 2023-01-23).
6
7
8 827 (62) Villamil, J. A.; Mohedano, A. F.; Rodriguez, J. J.; de la Rubia, M. A. Valorisation of
9
10 828 the Liquid Fraction from Hydrothermal Carbonisation of Sewage Sludge by Anaerobic
11
12 829 Digestion. *Journal of Chemical Technology and Biotechnology* **2018**, *93* (2), 450–456.
13
14 830 <https://doi.org/10.1002/jctb.5375>.
15
16
17
18 831 (63) Zhu, J.; Song, W.; Chen, X.; Sun, S. Integrated Process to Produce Biohydrogen from
19
20 832 Wheat Straw by Enzymatic Saccharification and Dark Fermentation. *Int J Hydrogen*
21
22 833 *Energy* **2022**. <https://doi.org/10.1016/J.IJHYDENE.2022.05.056>.
23
24
25
26 834 (64) Oliveira, A. S.; Sarrión, A.; Baeza, J. A.; Diaz, E.; Calvo, L.; Mohedano, A. F.;
27
28 835 Gilarranz, M. A. Integration of Hydrothermal Carbonization and Aqueous Phase
29
30 836 Reforming for Energy Recovery from Sewage Sludge. *Chemical Engineering Journal*
31
32 837 **2022**, *442*, 136301. <https://doi.org/10.1016/J.CEJ.2022.136301>.
33
34
35
36 838 (65) Medina-Martos, E.; Istrate, I. R.; Villamil, J. A.; Gálvez-Martos, J. L.; Dufour, J.;
37
38 839 Mohedano, Á. F. Techno-Economic and Life Cycle Assessment of an Integrated
39
40 840 Hydrothermal Carbonization System for Sewage Sludge. *J Clean Prod* **2020**, *277*,
41
42 841 122930. <https://doi.org/10.1016/J.JCLEPRO.2020.122930>.
43
44
45
46 842 (66) Vardanyan, A.; Kafa, N.; Konstantinidis, V.; Shin, S. G.; Vyrides, I. Phosphorus
47
48 843 Dissolution from Dewatered Anaerobic Sludge: Effect of PHs, Microorganisms, and
49
50 844 Sequential Extraction. *Bioresour Technol* **2018**, *249*, 464–472.
51
52 845 <https://doi.org/10.1016/J.BIORTECH.2017.09.188>.
53
54
55
56 846 (67) Munir, M. T.; Li, B.; Boiarkina, I.; Baroutian, S.; Yu, W.; Young, B. R. Phosphate
57
58 847 Recovery from Hydrothermally Treated Sewage Sludge Using Struvite Precipitation.
59
60 848 *Bioresour Technol* **2017**, *239*, 171–179. <https://doi.org/10.1016/j.biortech.2017.04.129>.

- 1
2
3 849 (68) Huang, H.; Huang, L.; Zhang, Q.; Jiang, Y.; Ding, L. Chlorination Decomposition of
4
5 850 Struvite and Recycling of Its Product for the Removal of Ammonium-Nitrogen from
6
7 851 Landfill Leachate. *Chemosphere* **2015**, *136*, 289–296.
8
9
10 852 <https://doi.org/10.1016/J.CHEMOSPHERE.2014.10.078>.
11
12
13 853 (69) Sarrion, A.; Ipiates, R. P.; de la Rubia, M. A.; Mohedano, A. F.; Diaz, E. Chicken Meat
14
15 854 and Bone Meal Valorization by Hydrothermal Treatment and Anaerobic Digestion:
16
17 855 Biofuel Production and Nutrient Recovery. *Renew Energy* **2023**.
18
19
20 856 <https://doi.org/10.1016/J.RENENE.2023.01.005>.
21
22
23 857 (70) Daneshgar, S.; Buttafava, A.; Callegari, A.; Capodaglio, A. G. Economic and Energetic
24
25 858 Assessment of Different Phosphorus Recovery Options from Aerobic Sludge. *J Clean*
26
27 859 *Prod* **2019**, *223*, 729–738. <https://doi.org/10.1016/J.JCLEPRO.2019.03.195>.
28
29
30 860 (71) Wang, L.; Chang, Y.; Li, A. Hydrothermal Carbonization for Energy-Efficient
31
32 861 Processing of Sewage Sludge: A Review. *Renewable and Sustainable Energy Reviews*
33
34 862 **2019**, *108*, 423–440. <https://doi.org/10.1016/J.RSER.2019.04.011>.
35
36
37
38 863
39
40
41 864
42
43



44
45
46
47
48
49
50
51
52 865
53
54
55 866
56
57
58 867
59
60

“For Table of Contents Use Only”

1
2
3 868 **Synopsis:** Scheme of the different hydrothermal treatment routes of digested sewage sludge
4
5 869 for nutrient solubilization and their subsequent recovery as struvite.
6
7
8
9
10
11
12
13
14
15
16
17
18
19
20
21
22
23
24
25
26
27
28
29
30
31
32
33
34
35
36
37
38
39
40
41
42
43
44
45
46
47
48
49
50
51
52
53
54
55
56
57
58
59
60